SOCIAL INTERACTION, VOLATILITY CLUSTERING, AND MOMENTUM

XUE-ZHONG HE[†], KAI LI[‡], CATERINA SANTI[§] AND LEI SHI[‡]

[†]University of Technology Sydney

[‡]Macquarie University

[§]University College Cork

tony.he1@uts.edu.au, kai.li@mq.edu.au, caterina.santi@ucc.ie, l.shi@mq.edu.au

Abstract. This paper incorporates information uncertainty and social interaction among investors into a random utility framework and develops an evolutionary equilibrium model of asset pricing and investor choice dynamics. We show that strong social interaction can lead to endogenous switching between two persistent regimes for the mean choice and return volatility, which can simultaneously generate time-series momentum and volatility clustering in asset returns. By using StockTwits post volume as a proxy for social interaction, we provide empirical evidence for the model predictions for various equity indices.

Keywords: Social interaction, mean choice, volatility clustering, time-series momentum.

JEL Classification: G02, G12, G14

Date: April 19, 2021.

Acknowledgments: We would like to thank Nihad Aliyev, Youwei Li, Jun Liu, George Tauchen, Marco Tolotti, Jun Tu, Huanhuan Zheng, Qiaoqiao Zhu, Xiaoyu Zong and conference and seminar participants at the 2014 Sydney Economics and Financial Market Workshop, the 2015 Conference on Computing in Economics and Finance (Taipei), the 2016 China International Conference in Finance, the 2016 International Conference on Nonlinear Economic Dynamics (Tokyo), the 2016 International Conference on Applied Financial Economics (Shanghai), Ca' Foscari University of Venice, Australian National University, Nankai University, Sun Yet-sen University, Tianjin University, and University of Technology Sydney for helpful comments and suggestions. Financial support from the Australian Research Council (ARC) under Discovery grants (DP130103210 and DE180100649) and a National Natural Science Foundation of China (NSFC) grant (No 71320107003) is gratefully acknowledged. The usual caveats apply.

Social Interaction, Volatility Clustering, and Momentum

Abstract

This paper incorporates information uncertainty and social interaction among investors into a random utility framework and develops an evolutionary equilibrium model of asset pricing and investor choice dynamics. We show that strong social interaction can lead to endogenous switching between two persistent regimes for the mean choice and return volatility, which can simultaneously generate time-series momentum and volatility clustering in asset returns. By using StockTwits post volume as a proxy for social interaction, we provide empirical evidence for the model predictions for various equity indices.

Keywords: Social interaction, mean choice, volatility clustering, time-series momentum.

JEL Classification: G02, G12, G14

1. Introduction

Two stylized facts about asset returns in equity markets have puzzled finance researchers: namely, volatility clustering and time-series momentum. First, volatility clustering refers to the fact that large (small) price changes tend to be followed by large (small) price changes of either sign. It was first noted by Mandelbrot (1963) and is widely observed in financial markets.[1] With notable asset pricing implications, volatility clustering is the focal point of investment and risk management. The widespread ARCH and GARCH models[2] provide rich econometric techniques to characterize these features and have motivated various efforts to provide theoretical explanations. However, these explanations are often exogenous, relying on exogenous time-varying preferences, persistent information arrival, and heterogeneous trading frequency, sometimes introducing volatility regime shifts directly.[3] Second, time-series momentum, that is, the strong positive predictive ability of a security's own past returns, has been documented and explored by Moskowitz, Ooi and Pedersen (2012). Explanations for short-run momentum and long-run reversal are often based on behavioral theories.[4]

Motivated by recent studies linking social interaction to investor trading behavior, we propose the social interaction of investors as an *endogenous* explanation for volatility clustering. By incorporating uncertainty from noisy signals on fundamentals and social interaction of investors into a random utility framework, we develop an equilibrium model of asset pricing and population dynamics of investor mean choice. We show that driven by the peer-group effect from strong social interaction, the mean choice can switch between two persistent regimes: the high mean choice regime is characterized as a regime with a more informative asset price and hence low return volatility, while the low mean choice regime displays a less informative asset price and hence high return volatility. With the persistence of the mean choice in each regime, large shocks to fundamental and public signals can occasionally trigger endogenous switches between the two regimes, generating volatility clustering. Moreover, this type of endogenous switching can also generate the

[1] More explicitly, "*returns...have surprisingly large numbers of extreme values, and both the extremes and quiet periods are clustered in time*" (Engle, 2004).

[2] See, e.g., Engle (1982), Bollerslev (1986), and Engle (2004).

[3] See, e.g., Hamilton and Susmel (1994), Andersen and Bollerslev (1997), Muller et al. (1997), Cao et al. (2002), Engle (2004), Marquering and Verbeek (2004) and Fleming et al. (2006).

[4] See, for example, Barberis, Shleifer and Vishny (1998), Daniel, Hirshleifer and Subrahmanyam (1998) and Hong and Stein (1999).

time-series momentum characterized by the short-term predictive ability of a security's own past returns at the monthly level. Using StockTwits post volume as a proxy for social interaction, we provide empirical evidence on the model predictions on volatility clustering and time-series momentum for various equity indices.

Fundamental information is noisy. The informativeness of the observed noisy fundamental information can be either high or low. In equilibrium, the mean choice refers to investors' average choice of beliefs about this informativeness. When investors update their beliefs based on perceived fundamental innovations, they adapt their behavior through social interaction, with a peer-group effect inducing a tendency for conformity in behavior across investors. Following the static random utility approach of Brock and Durlauf (2001) and the dynamical population game model of Blume (2003) and Blume and Durlauf (2003), we model the mean choice as a stochastic process of individuals' response, where investors adapt their own strategic choice to that of the population. Thus, the steady states of a deterministic approximation of the stochastic model are characterized by the static Nash equilibria of the mean choice. When social interaction is weak (below a threshold value), there exists a unique (symmetric) steady state for the mean choice, and investors' choices are equally divided. However, when social interactions are strong (above the threshold value), the peer effect of social interaction generates two additional (asymmetric) steady states. More importantly, with increasing social interaction, the change in stability from the symmetric steady state to the two asymmetric steady states reflects the (local) persistence of the mean choice in each regime. Intuitively, when one choice is made by the majority of investors, it becomes more attractive for individual investors. We also follow Blume (2003) and introduce a relative performance measure based on the prediction errors as the private utility component in the random utility framework, which we refer to as private utility shocks. With the combination of the (local) persistence of the mean choice in each regime, fundamental shocks and public signals then trigger endogenous regime switching in the population's choice dynamics.

In equilibrium, the asset price is the population-weighted average equilibrium price under investors' choice of beliefs. When one choice is made by the majority of investors, they pull the price to their own valuation. Therefore, the mean choice affects price informativeness and hence asset return volatility. With strong social interaction, a high mean choice leads to a low-volatility regime, where the majority of investors choose to believe that the public signal is relatively more informative. As the aggregate market perceives less uncertainty, asset returns are less volatile. On the other hand, a low mean choice leads to a high-volatility regime, where the majority of investors choose to believe that the public signal is relatively less informative. Hence, asset returns are more volatile. Consequently, endogenous regime switching in the population's choice dynamics results in endogenous regime switching in asset return volatility. Hence, social interaction can serve as an endogenous mechanism driving the phenomenon of volatility clustering; i.e., return volatility is serially correlated and switches between a high and a low regime.

Moreover, the switching intensity between the two regimes increases in the sensitivity to private utility shocks, and the difference in volatility between the two regimes increases in belief dispersion and social interaction. This is because high sensitivity to private utility shocks enlarges the magnitude of their effect, which causes investors' mean choice to switch more often. Additionally, strong social interaction leads to a more polarized mean choice, which, coupled with large dispersion in beliefs about informativeness, results in a greater difference in volatility between the two regimes. Therefore, social interaction in a random utility framework provides a microfoundation for the endogenous switching of investors' beliefs as well as the switching intensity.

The mechanism behind volatility clustering also has implications for time-series momentum, that is, the predictive ability of a security's own past returns at the monthly level. By examining the autocovariance of asset returns, we find that when the mean choice is persistent over short time horizons, the market price maintains a price trend driven by the dominating group of investors, resulting in time-series momentum in the short run. Therefore, social interaction also serves as an underlying mechanism for this return predictability.

Finally, using data from StockTwits, a social media investing platform, we provide an empirical validation of the theoretical model predictions. We observe that the autocorrelation of volatility is significantly higher when social interaction is strong. A GARCH analysis further shows significant volatility clustering with strong social interaction. We also find that the returns of time-series momentum portfolios are significantly positive when social interaction is strong but negative when social interaction is weak.

1.1. **Related Literature.** Our paper is closely related to a diverse literature on social interaction and its implications for asset returns and investor choice dynamics in financial markets.

Our first contribution to the literature is to present social interaction as a novel channel of information uncertainty in asset pricing. The importance of social interaction based on the peer effect in various aspects of investing has been well documented in the literature and explains a variety of phenomena in financial markets.[5] The literature also explores the impact of social interactions on portfolio choice.[6] The theoretical literature suggests several factors giving rise to herding.[7] Recent empirical studies demonstrate that social interaction can increase active trading, affect investors' investment and debt decision making and contribute significantly to the disposition effect (Heimer, 2016).[8] Instead of focusing on the mechanism that gives rise to the peer effect, we posit social interaction as a mechanism driving the mean choice and hence the informativeness of observed noisy fundamental information. We show that with information uncertainty, the level of market informativeness, and hence return volatility, can be characterized by endogenous switching in the mean choice between different regimes.

Second, this paper complements the literature that examines the nonlinear impact of heterogeneity and social interaction on aggregate outcomes, particularly through multiple steady states of market equilibrium. The pervasiveness of heterogeneity and social interaction in economics has been well documented.[9] With noisy fundamental information, investors face uncertainty regarding its informativeness. Considering either fixed types or

[5]For example, Hong et al. (2004) show that households that are more socially active are also more likely to invest in the stock market. Kaustia and Knüpfer (2012) present evidence of outcome-based influence and show that local peers' recent experience with stock returns affects an individual's stock market entry decision, particularly in areas with better opportunities for social learning.

[6]Hong et al. (2005) show that mutual fund managers tend to buy stocks that their local peers have bought in the recent past.

[7]Scharfstein and Stein (1990) attribute it to reputation concerns and the unpredictable components to investment outcomes. Another well-known example is the information cascades of Banerjee (1992) and Bikhchandani et al. (1992), whereby investors who have imperfect information optimally give some weight to prior investors' decisions. Shiller (1995) argues that the differences across groups in herding behavior may be more due to differences in the nature of information transmission.

[8]In related studies, Feng and Seasholes (2004) provide evidence when dividing investors geographically in China that trades are highly correlated. In Finland, Shive (2010) shows that social learning is a significant predictor of stock market trading. In the US, Ivković and Weisbenner (2007) find that investors are more likely to purchase stocks from a particular industry if their neighbors purchase stocks from that industry. Welch (2000) finds that analysts are more likely to revise their recommendations toward prior consensus recommendations than away from them. Jegadeesh and Kim (2010) indicate that analysts' recommendation revisions are partly driven by their tendencies to herd. Han and Hirshleifer (2012) demonstrate that social interaction contributes to the growth of active strategies.

[9]See, e.g., Keynes (1936), Becker (1974), Heckman (2001), and Brock and Durlauf (2001).

constant population fractions of heterogeneous investors, the rational expectations equilibrium asset pricing literature falls short in capturing the effect of time-varying population characteristics and hence the informativeness of noisy fundamentals for asset pricing.[10] In this paper, we follow Brock and Durlauf (2001), Blume (2003) and Blume and Durlauf (2003) to model the time-varying mean choice of the investor population. The resulting nonlinear model can have multiple steady states. Driven by the relative performance of investors in their private utility component, the nonlinear interaction of the time-varying investor choice with the market price can lead to endogenous switching between different steady states. This provides a simple mechanism to explore more complicated market behavior than the traditionally linear equilibrium can rationalize. Furthermore, social interaction provides a microfoundation for endogenous switching and switching intensity for models in which switching is typically assumed exogenous (see, e.g., Hamilton and Susmel, 1994).

Third, this paper posits social interaction as a novel economic explanation for the stochastic volatility, particularly volatility clustering, that is empirically described by the (G)ARCH model and its extensions (Engle, 1982, Bollerslev, 1986). GARCH models have offered econometric tools to successfully explain volatility dynamics (Engle, 2004). Some models have been developed to explore the economic mechanisms underlying stochastic volatility by introducing, for example, volatility regime shifts directly (Hamilton and Susmel, 1994), persistence in exogenous information arrival (Engle, 2004; Andersen and Bollerslev, 1997; Cao et al, 2002; Fleming et al, 2006), heterogeneous trading frequency (Muller et al, 1997), parameter uncertainty (Johnson, 2001), and time-varying risk aversion (McQueen and Vorkink, 2004). In contrast to these exogenous approaches, this paper posits social interaction as an endogenous mechanism behind volatility clustering.

Fourth, this paper offers an approach different from that of heterogeneous agent models (HAMs) in explaining volatility clustering. From a complex systems perspective, HAMs assume heterogeneous (e.g., fundamental and trend-following) expectations and model the heuristic switching of agents based on the performance of different trading strategies.[11] By examining the impact of the nonlinearity on complex price behavior, HAMs can explain

[10]See, e.g., Dumas, Kurshev and Uppal (2009) and Cao and Ou-Yang (2009).

[11]We refer to Hommes (2006), LeBaron (2006), Chiarella, Dieci and He (2009), and Dieci and He (2018) for surveys in this literature.

various stylized facts, including volatility clustering and market anomalies.[12] Instead of assuming exogenous heuristic switching, we provide an endogenous switching mechanism through Nash equilibrium in this paper.

Finally, this paper also offers a complementary explanation of short-run time-series momentum, which has mostly been explained based on certain behavioral theories in the literature.[13] Moskowitz et al. (2012) empirically investigate time-series momentum defined by a strong positive predictive ability of a security's own past returns. Complementarily to this literature, we posit endogenous regime switching via a social interaction channel as an explanation for time-series momentum. In the different regimes, the asset price maintains a price trend driven by the dominant group of investors. Buffeted by noisy signals, asset prices fluctuate persistently and switch stochastically between different regimes, resulting in time-series momentum in the short run.

The paper is organized as follows. We first develop an evolutionary equilibrium of the asset price and investor choice dynamics in Section 2. Section 3 focuses on the choice dynamics. Regime switching and volatility clustering are examined in Section 4, while time-series momentum is studied in Section 5. Section 6 presents the empirical analysis, and Section 7 concludes. All the proofs, additional analyses, and empirical background are provided in the Appendices.

2. The Model

Consider an economy with two assets: a risk-free asset in perfectly elastic supply with a constant interest rate r and a risky asset in zero net supply that pays dividend $D_t dt$ over a time interval $[t, t + dt]$. The dividend follows

$$dD_t = f_t dt + \sigma_D dZ_{D,t}, \tag{1}$$

where σ_D is a constant, $Z_{D,t}$ is a standard Wiener process, and f_t follows a mean-reverting process

$$df_t = \lambda(\bar{f} - f_t)dt + \sigma_f dZ_{f,t}, \tag{2}$$

[12]See, e.g., Lux (1995), Brock and Hommes (1997*a*), Brock and Hommes (1998), Lux and Marchesi (1999), Chiarella and He (2002), LeBaron (2006), Gaunersdorfer and Hommes (2007), He and Li (2007, 2015*b*, 2015*a*), Di Guilmi et al. (2014), and He et al. (2016).

[13]Barberis et al. (1998) argue that momentum is the result of systematic errors that investors make when they use public information to form expectations about future cash flows. The models of Daniel et al. (1998) with a single representative investor and Hong and Stein (1999) with different trader types attribute the underreaction to overconfidence and the overreaction to biased self-attribution.

where $\lambda \geq 0$ measures the speed of mean reversion, $\bar{f}$ is the long-run mean, σ_f is the constant volatility of f_t, and $Z_{f,t}$ is a standard Wiener process independent of $Z_{D,t}$. We assume that f_t represents the *fundamental state* of the economy, which is unobservable to investors.

There is a continuum of investors, indexed by $i \in (0,1)$, who observe the dividend changes dD_t and a public signal s_t, which follows

$$ds_t = \sigma_s \rho dZ_{f,t} + \sigma_s \sqrt{1-\rho^2} dZ_{s,t}. \tag{3}$$

When $\rho > 0$, the public signal s_t is informative about the fundamental state f_t, where ρ measures the level of informativeness. When $\rho = 1$, s_t fully reveals f_t. On the other hand, s_t is purely noise when $\rho = 0$. We assume that investors may disagree about the informative parameter ρ.

2.1. **Information Uncertainty and Investors' Beliefs.** We assume that at time t, investors can choose between two different beliefs about the fundamental, namely, $\hat{f}_t^A$ and $\hat{f}_t^B$, that characterize the uncertainty about the informativeness of the public signal. Let ϕ_t denote the population fraction of investors who choose belief $\hat{f}_t^A$ and $1-\phi_t$ the fraction of those who choose belief $\hat{f}_t^B$. Moreover, each belief, $\hat{f}_t^k$, $k = A, B$, about the fundamental state is based on the Bayesian updating rule,

$$d\hat{f}_t^k = \lambda(\bar{f} - \hat{f}_t^k)dt + \frac{\gamma_k}{\sigma_D} dZ_{D,t}^k + \rho_k \sigma_f dZ_{s,t}, \tag{4}$$

where ρ_k is the signal informativeness. We assume that $\rho_A = \rho(1+\epsilon)$ and $\rho_B = \rho(1-\epsilon)$, with $\epsilon \geq 0$ measuring the degree of disagreement.[14] Furthermore,

$$dZ_{D,t}^k = \frac{dD_t - \hat{f}_t^k dt}{\sigma_D}, \qquad dZ_{s,t} = \frac{ds_t}{\sigma_s}, \tag{5}$$

are independent Wiener increments, and the variance of the stationary distribution for $\hat{f}_t^k$ is given by

$$\gamma_k = \left[\sqrt{\lambda^2 + (1-\rho_k^2)\sigma_f^2/\sigma_D^2} - \lambda\right]\sigma_D^2, \qquad k = A, B. \tag{6}$$

The following subsections examine how investors make their portfolio and belief choices. At time t, each investor i follows a two-stage process to select her belief $\hat{f}_t^i$ about the fundamental and optimal portfolio x_t^i (number of shares held in the risky asset). We first describe the portfolio selection process.

[14]We choose a mean-spread symmetric dispersion of the informativeness to highlight the effect of the degree of the dispersion; the results hold for any choices of ρ_A and ρ_B.

2.2. **Portfolio Choices and Equilibrium Price.** At the portfolio selection stage, we take investor i's belief choice $\hat{f}_t^i$ as given, i.e., $\hat{f}_t^i = \hat{f}_t^A$ or $\hat{f}_t^B$. To simplify the exposition, we first consider a discrete-time model with time increment Δt between periods t and $t+1$; then, we take the continuous-time limit as $\Delta t \to 0$.

Assume investor i maximizes a mean-variance utility over the next period's wealth; i.e., investor i's objective is

$$\max_{x_t^i} \mathbb{E}_t^i \left[W_{t+1}^i\right] - \frac{1}{2}\gamma \mathbb{V}ar_t^i \left[W_{t+1}^i\right], \tag{7}$$

where

$$W_{t+1}^i = RW_t^i + x_t^i \left(P_{t+1} + D_{t+1} - RP_t\right)$$

is the portfolio wealth, $R = 1 + r\Delta t$, and P_t is the market price of the risky asset. Then, the optimal demand of investor i for risky asset x_t^{i*} is given by

$$x_t^{i*} = \frac{\mathbb{E}_t^i \left[P_{t+1} + D_{t+1} - RP_t\right]}{\gamma \mathbb{V}ar_t^i \left[P_{t+1} + D_{t+1} - RP_t\right]}. \tag{8}$$

We assume a common conditional variance of excess return, i.e.,

$$\mathbb{V}ar_t^i \left[P_{t+1} + D_{t+1} - RP_t\right] = \sigma_t^2 \Delta t,$$

where σ_t^2 is the annualized variance. Moreover, we assume that each investor forms her expectation about the next-period payoff as

$$\mathbb{E}_t^i \left[P_{t+1} + D_{t+1}\right] = RP_t + \kappa_t \left(P_t^i - P_t\right) \Delta t, \tag{9}$$

where P_t^i is equal to either P_t^A or P_t^B and

$$P_t^k = \sum_{s=1}^{\infty} \mathbb{E}_t^k \left[\frac{D_{t+s}}{R^s}\right], \qquad k = A, B \tag{10}$$

is the equilibrium price should everyone subscribe to belief $\hat{f}_t^k$ about the fundamental state. Intuitively, with information uncertainty, investors have heterogeneous valuations of the risky asset, and they seek to learn about their own valuation by making inferences from the equilibrium price. Consequently, investor i expects the equilibrium price to revert back to what she currently believed the fundamental price to be over the time interval $[t, t + \Delta t]$, and the speed of mean reversion is $\kappa_t \Delta t$. Under (9), investor i's optimal portfolio is given by

$$x_t^{i*} = \frac{\kappa_t}{\gamma \sigma_t^2} \left(P_t^i - P_t\right). \tag{11}$$

By the market clearing condition, $\phi_t x_t^{A*} + (1 - \phi_t) x_t^{B*} = 0$, the equilibrium price is given by

$$P_t = \phi_t P_t^A + (1 - \phi_t) P_t^B. \tag{12}$$

When we take the continuous-time limit as $\Delta t \to 0$, we obtain

$$P_t^k = \mathbb{E}_t^k\left[\int_t^\infty e^{-r(s-t)} D_s ds\right] = \frac{D_t}{r} + \frac{1}{r^2}\left[\frac{r}{r+\lambda}\hat{f}_t^k + \frac{\lambda}{r+\lambda}\bar{f}\right], \qquad k = A, B. \tag{13}$$

The intuition behind the weighted average of prices in (12) is as follows. Investors who are more optimistic (pessimistic) about the fundamental state take a long (short) position in the stock. Therefore, when the market fraction increases for optimistic (pessimistic) investors, they pull the price closer to their valuation, and the equilibrium price must increase (decrease) to clear the market.

2.3. **Belief Choices and Market Fractions.** Next, we model investors' *belief choice* in the first stage, i.e., how investors choose between beliefs $\hat{f}_t^A$ and $\hat{f}_t^B$ about the fundamental state, and determine the population fraction ϕ_t. Each investor i at time t makes a binary choice $\omega_t^i \in \{-1, 1\}$, in which $\omega_t^i = 1$ corresponds to the choice of $\hat{f}_t^i = \hat{f}_t^A$ while $\omega_t^i = -1$ corresponds to the choice of $\hat{f}_t^i = \hat{f}_t^B$. Therefore we can use

$$m_t \equiv \int_0^1 \omega_t^i di \tag{14}$$

to measure the *mean choice* of investors. Note that $\phi_t = (1 + m_t)/2$. With a high (low) mean choice, a majority of the investors believe that the public signal, s_t, is more (less) informative about the fundamental state, f_t.

We follow the random utility model of Brock and Durlauf (2001) to decompose investor i's utility into three components; that is, investor i's preference over ω^i is given by

$$u^i(\omega^i) = (h\omega^i + k) + J\omega^i m^i + \xi^i(\omega^i). \tag{15}$$

The first component $h\omega^i + k$ measures *private utility*. The second component, $J\omega^i m^i$, measures *social utility*, where m^i is investor i's expectation of the mean choice level. Intuitively, when $J > 0$, investor i has an incentive to conform to the mean choice. The third component, $\xi^i(\omega^i)$, measures *random utility*, which generates heterogeneity among investors.

A key result from Brock and Durlauf (2001) is that when the random utility component satisfies

$$\mathbb{P}(\xi^i(-1) - \xi^i(1) \le x) = \frac{1}{1 + e^{-\beta x}}, \qquad x > 0, \qquad \beta > 0, \tag{16}$$

the probability of which choice investor i makes is then characterized by the discrete-choice model

$$\mathbb{P}(\omega^i | m^i) = \frac{e^{\beta\omega_t^i(h+Jm^i)}}{e^{\beta\omega^i(h+Jm^i)} + e^{-\beta\omega^i(h+Jm^i)}}, \qquad \omega^i \in \{-1, 1\} \tag{17}$$

while the mean choice level is given by

$$m = 1 \cdot \mathbb{P}(\omega^i = 1) + (-1) \cdot \mathbb{P}(\omega^i = -1) = \tanh[\beta(h + Jm)]. \tag{18}$$

To develop a dynamic model for mean choice m_t, we follow Blume and Durlauf (2003) and transpose (17) into an independent Poisson process with switching rate[15]

$$\eta_t^i \equiv \lim_{s \to 0} \frac{1}{s} \mathbb{P}(\omega_{t+s}^i \neq \omega_t^i | \omega_t^i, m_t) = e^{-\beta \omega_t^i (h_t + Jm_t)}, \tag{19}$$

where m_t is the current mean choice level and h_t measures the relative accuracy of beliefs $\hat{f}_t^A$ and $\hat{f}_t^B$ at time t. Intuitively, investor i is more likely to switch her choice when $\omega_t^i(h_t + Jm_t) < 0$, i.e., when her current choice either does not align with the mean choice level or does not align with the realized dividends and public signals (and hence private utility is relatively low). Motivated by Brock and Durlauf (2001), we choose

$$h_t = b(\delta_t^B - \delta_t^A), \tag{20}$$

where parameter $b \geq 0$ measures sensitivity to the relative accuracy parameter and[16]

$$\delta_t^k = \Big[\frac{1}{\theta} \int_{t-\theta}^t dD_u - \hat{f}_t^k\Big]^2 = \Big[\frac{D_t - D_{t-\theta}}{\theta} - \hat{f}_t^k\Big]^2, \qquad k = A, B. \tag{21}$$

The idea behind (20) and (21) is simple. A choice is relatively more accurate if the inferred fundamental state $\hat{f}_t^k$ has a smaller realized (squared) error from the average change in dividends $(D_t - D_{t-\theta})/\theta$ over a moving time horizon $\theta\,(> 0)$. In particular, investors consider all historical dividends when $\theta \to \infty$ but only the current dividend surprise when $\theta \to 0$.

Corresponding to the switching rate of investor i's choice in (19), Blume and Durlauf (2003) derive the following mean choice dynamics of the investor population,

$$\frac{dm_t}{dt} = \tanh\big[\beta(h_t + Jm_t)\big] - m_t, \tag{22}$$

which has the same steady states of the static Nash equilibrium (18).[17]

[15]We refer the reader to Barucci and Tolotti (2012) for a general discussion on this dynamic decision process when agents are heterogeneous with a time-varying degree of conformism.

[16]Alternatively, we can replace $(D_t - D_{t-\theta})/\theta$ with $M_t = \int_{t-\infty}^t e^{-\iota(t-u)} dD_u$, which satisfies $dM_t = dD_t - M_t dt$ when $\iota = 1$. We can show that the main results still hold with this choice.

[17]Instead of the relative accuracy h_t, (17) reduces to the discrete-choice model where investors update their choices based on some fitness measure (see, e.g., Brock and Hommes, 1997*b*; He and Li, and 2012).

2.4. **Equilibrium Return Dynamics.** From (11), (22), and $\phi_t = (1 + m_t)/2$, we see that the equilibrium price is the population-weighted average of the fundamental values perceived by investors. Next, we characterize the dynamics of the instantaneous asset return. Note that the perceived expected instantaneous return varies across investors due to their different beliefs about the fundamental state. In the following, we assume an objective belief f_t^*, which is based on the true informativeness parameter ρ, with

$$d\hat{f}_t^* = \lambda(\bar{f} - \hat{f}_t^*)dt + \frac{\gamma^*}{\sigma_D} dZ_{D,t}^* + \rho\sigma_f dZ_{s,t}^*, \tag{23}$$

where

$$dZ_{D,t}^* = \frac{dD_t - \hat{f}_t^* dt}{\sigma_D}, \qquad dZ_{s,t}^* = \frac{ds_t}{\sigma_s} \tag{24}$$

and

$$\gamma^* = \left[\sqrt{\lambda^2 + (1-\rho^2)\sigma_f^2/\sigma_D^2} - \lambda\right]\sigma_D^2. \tag{25}$$

The return dynamics are then given by

$$dR_t = dP_t + D_t dt = (rP_t + \mu_t)dt + V_{D,t} dZ_{D,t}^* + V_{s,t} dZ_{s,t}^*, \tag{26}$$

where μ_t measures the risk premium and $V_{D,t}$ and $V_{s,t}$ are the volatility coefficients.

When $\epsilon = 0$ and all investors subscribe to belief $\hat{f}_t^*$ about the fundamental state based on informativeness ρ, we have a *benchmark price*

$$P_t^* = \frac{D_t}{r} + \frac{1}{r^2}\left[\frac{r}{r+\lambda}\hat{f}_t^* + \frac{\lambda}{r+\lambda}\bar{f}\right], \tag{27}$$

and the return dynamics follow

$$dR_t = rP_t dt + \left[\frac{\sigma_D}{r} + \frac{\gamma^*}{r(r+\lambda)\sigma_D}\right] dZ_{D,t}^* + \frac{\sigma_f \rho}{r(r+\lambda)} dZ_{s,t}^*. \tag{28}$$

The assumption of an objective informativeness coefficient that differs from ρ_A and ρ_B reflects the uncertainty about the informativeness of the observed noisy fundamental. This assumption is important to ensure the long-run stationarity of the mean choice distribution. Suppose that either ρ_A or ρ_B coincides with ρ; then, in the long run, one would expect the private utility component to dominate investors' choices, and eventually all investors' belief choices about the fundamental state would converge to either $\hat{f}_t^A$ or $\hat{f}_t^B$. Therefore, to ensure long-run heterogeneity, we assume that the true value lies somewhere in between, i.e., $\rho_B < \rho < \rho_A$ (for $\epsilon > 0$). The following proposition fully characterizes the equilibrium return dynamics with respect to the risk premium μ_t and volatilities $V_{D,t}$ and $V_{s,t}$.

Proposition 2.1. *The instantaneous return of the risky security follows* (26)*, where the risk premium and the volatility coefficients are given by*

$$\mu_t = \underbrace{\frac{1}{r}\left\{\left[1+\frac{\gamma_A}{\sigma_D^2(r+\lambda)}\right]\phi_t(\hat{f}_t^* - \hat{f}_t^A) + \left[1+\frac{\gamma_B}{\sigma_D^2(r+\lambda)}\right](1-\phi_t)(\hat{f}_t^* - \hat{f}_t^B)\right\}}_{\textit{heterogeneous-beliefs}}$$

$$+ \underbrace{\frac{1}{2r(r+\lambda)}(\hat{f}_t^A - \hat{f}_t^B)\left\{\tanh\left[\beta[h_t + Jm_t]\right] - m_t\right\}}_{\textit{social-interactions}}, \tag{29}$$

$$V_{D,t} = \frac{\sigma_D}{r} + \frac{1}{r(r+\lambda)\sigma_D}[\phi_t\gamma_A + (1-\phi_t)\gamma_B], \tag{30}$$

$$V_{s,t} = \frac{\sigma_f}{r(r+\lambda)}[\phi_t\rho_A + (1-\phi_t)\rho_B] = \frac{\sigma_f\rho}{r(r+\lambda)}[1+m_t\epsilon], \tag{31}$$

where $\phi_t = \frac{1}{2}(1+m_t)$ *and the mean choice* m_t *follows* (22)*, with* h_t *defined in* (20)*.*

Proposition 2.1 implies that the *risk premium* μ_t in (29) consists of two components, namely, a *heterogeneous beliefs* component and a *social interaction* component. The former is positive (negative) when the mean choice-weighted average belief is overly pessimistic (overly optimistic). In contrast, the second component is independent of $\hat{f}_t$, and its contribution to the risk premium depends on the product $(\hat{f}_t^A - \hat{f}_t^B)d\phi_t$. Intuitively, a positive risk premium is expected when the mean choice moves toward the relatively more optimistic belief.

The equilibrium return dynamics in Proposition 2.1 show the dependence of the risk premium and volatility on the mean choice m_t. In the following sections, we first analyze the mean choice dynamics in the population and the stationarity of the mean choice distribution and then explore the implications for volatility persistence, regime switching, volatility clustering, and time-series momentum.

3. Population's Choice Dynamics

This section first provides results on the existence and stability of multiple steady states of the mean choice in the absence of private utility, as in Brock and Durlauf (2001). By considering random shocks to private utility, we then numerically examine the long-run stationarity of the population's dynamic mean choice distribution.

3.1. **Multiple Steady States and Regimes.** To better understand the mean choice dynamics in the population in (22), we first consider a special case without private utility (i.e., $b = 0$ and hence $h_t = 0$ in (20)). In this case, Brock and Durlauf (2001) show that the symmetric steady state is the unique equilibrium of (18) when $\beta J \leq 1$. However, when

$\beta J > 1$, there are two additional asymmetric equilibria. In the dynamic setting, the choice dynamics in the population are determined by an ordinary differential equation (ODE)

$$\frac{dm_t}{dt} = \tanh(\beta J m_t) - m_t, \tag{32}$$

which shares the same steady states but with different stability levels, summarized in the following corollary.

Corollary 3.1. *(Existence and stability of multiple equilibria) The mean choice dynamics of the population* (32) *have*

(i) *a unique steady state $m_0^* = 0$, which is globally asymptotically stable, when $\beta J < 1$;*

(ii) *three steady states $m_+^* = m^* > 0$, $m_0^* = 0$ and $m_-^* = -m^* < 0$ when $\beta J > 1$ satisfying $\tanh(\beta J m^*) = m^*$ for $m^* > 0$; in addition, m_+^* and m_-^* are locally asymptotically stable, and $m_0^* = 0$ is unstable.*

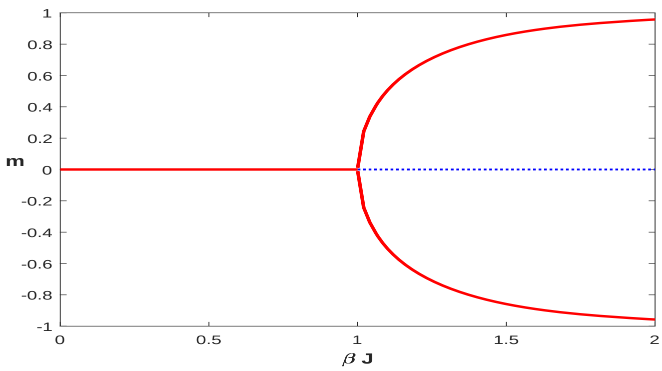

FIGURE 1. The steady states of the mean choice as functions of social interaction βJ and their stability, with (red) solid lines indicating stable and (blue) dotted lines indicating unstable steady states.

In the absence of private utility shocks, Corollary 3.1 shows that the symmetric equilibrium m_0^* is the unique and globally stable equilibrium when social interaction is weak ($\beta J < 1$). In this equilibrium, investors' choices among the two beliefs are equally divided. However, when social interaction is strong ($\beta J > 1$), the change in the stability of the symmetric equilibrium bifurcates, leading to two locally stable asymmetric equilibria, so that the mean choice converges to either $m_+^* > 0$ or $m_-^* < 0$, depending on its initial value. Intuitively, when one choice is made by the majority of investors, then it becomes more attractive for individual investors. This generates two regimes: at m_+^*, more investors choose to believe that the public signal is more informative about the fundamental, while at m^*_-, more investors choose to believe that the public signal is less informative about the fundamental. The results are illustrated in Fig. 1, showing the steady states (or regimes) of the mean choice as a function of social interactions βJ, together with their stability.

3.2. **Stationarity of the Mean Choice.** With private utility ($b > 0$), the population's choice dynamics are affected by random shocks from the dividend and public signal. We now examine the long-run stationarity of the distribution of the population's choice dynamics in (22) by simulating random paths for ϕ_t. Indeed, we find that the distribution of ϕ_t across 100 paths becomes stationary (i.e., changes in the distribution become negligible) after a long period of time. With the baseline parameter values (unless stated otherwise) in Table 1, Fig. 2 reports the stationary distribution of ϕ_t at time $t > 2,000$ for four combinations of parameter values of J and b to show the joint impact of social interactions and private utility, leading to two observations.

Parameters	λ	σ_f	ρ	ϵ	$\bar{f}$	θ	σ_D	b	β	J	r
Values	1	0.05	0.5	0.9	0.05	5	0.05	100	1	1.15	0.05

Table 1. Baseline parameter values used in numerical simulations.

First, in regards to social interaction, Figs. 2 (a) and (b) show that with weak social interaction ($\beta J < 1$), the mean choice and hence ϕ_t have a unimodal distribution centred around $\phi^*_0 = 1/2$ (i.e., $m^*_0 = 0$). However, with strong social interaction ($\beta J > 1$), Figs. 2 (c) and (d) show that ϕ_t displays bimodal distributions, corresponding to the two mean choice regimes around the two steady states, consistent with the two locally stable steady states $m^*_\pm$ in Corollary 3.1 for $b = 0$.

Second, in regards to private utility, by comparing the left and right panels, Fig. 2 shows that the distribution of the market fraction is more dispersed for larger values of b, which is true for both the unimodal and bimodal cases. Intuitively, for small b, the social utility component tends to dominate the private utility component in affecting investors' choices in the long run. In this case, when social interaction is weak, due to global stability, ϕ_t is pulled toward the unique steady state. When social interaction is strong, ϕ_t converges to one of the two stable steady states, while switching happens occasionally when shocks to private utility, i.e., h_t, are sufficiently large. The dominance of social utility over private utility in general is demonstrated by the more peaked distributions in Figs. 2 (b) and (d), consistent with Corollary 3.1 for $b = 0$. In contrast, for large b, large private utility shocks

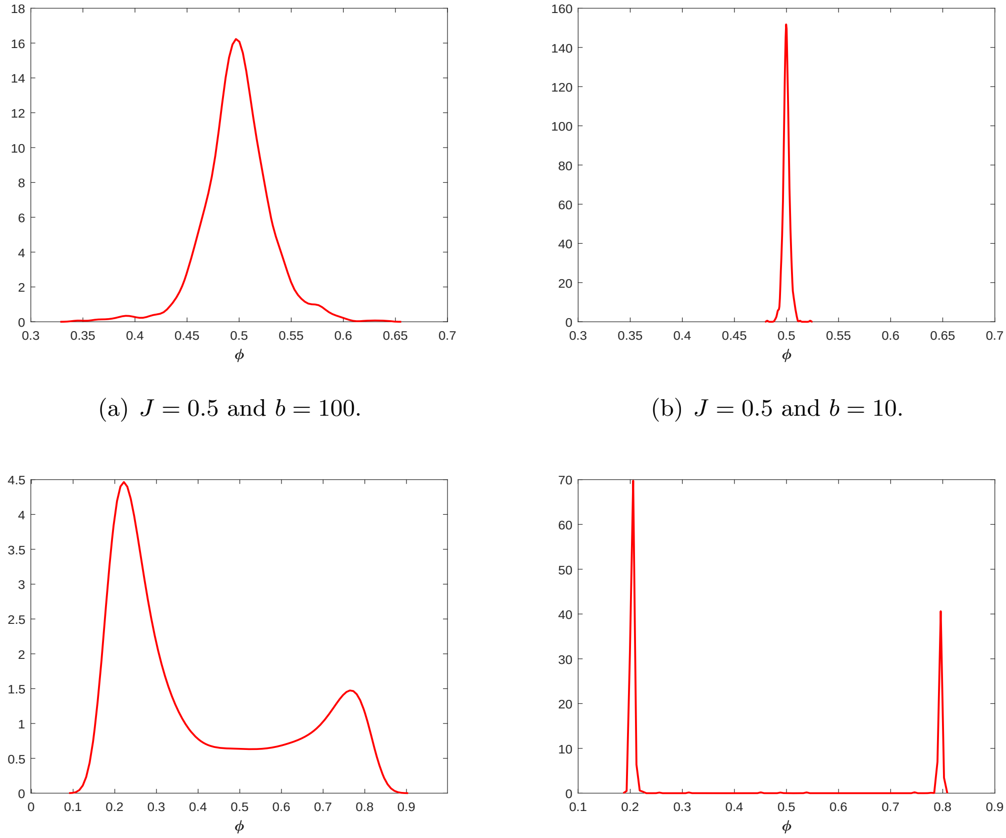

(a) $J = 0.5$ and $b = 100$.

(b) $J = 0.5$ and $b = 10$.

(c) $J = 1.15$ and $b = 100$.

(d) $J = 1.15$ and $b = 10$.

FIGURE 2. Distribution of ϕ_t for weak social interaction (a) and (b) ($J = 0.5(< 1)$) and strong social interaction (c) and (d) ($J = 1.15(> 1)$) for two values of $b = 10$ and 100. The other parameters are the same as in Table 1.

occur more frequently, which can potentially offset the social utility component, Jm_t, even when mean choice m_t is close to 1 or -1. Therefore, with weak social interaction, the tendency of ϕ_t towards the unique steady state is perturbed constantly by the shocks to private utility, characterized by a less peaked distribution in Fig. 2 (a) (in comparison with that in Fig. 2 (b)). When social interaction is strong, the perturbations of private utility shocks increase switching between the two regimes.[18] This is illustrated by more persistent switches among the two locally stable regimes in Fig. 2 (c) (in comparison with those in Fig. 2 (d)).

[18]More precisely, due to the continuous dynamic process in the population, *switching* here means a gradual transition, instead of a jump, between regimes. For convenience, we use the term *switching*, as in the regime-switching literature, this is not necessarily characterized by a jump in a process in general.

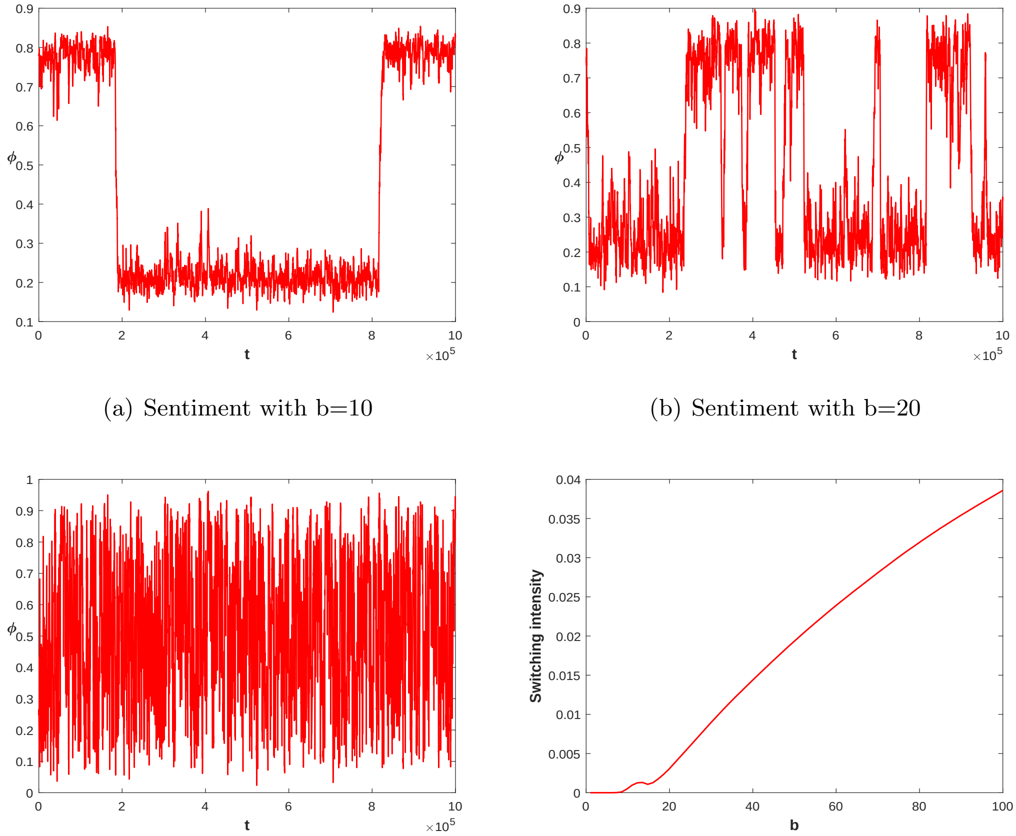

(a) Sentiment with b=10

(b) Sentiment with b=20

(c) Sentiment with b=100

(d) Switching intensity

FIGURE 3. Time series of mean choice for (a) $b = 10$, (b) $b = 20$, (c) $b = 100$, and (d) the switching intensity with respect to b; the other parameters are given by Table 1.

3.3. **Regime Switching.** With strong social interactions, the mean choice m_t is characterized by two locally stable regimes. The length of each switching cycle, i.e., the time that it takes to switch from one steady state to another, depends on the size of private utility shocks, which is controlled by b, and the basin of attraction for each regime. Fig. 3 (a) shows that for $b = 10$, the market fraction ϕ_t rarely switches between regimes. With small fundamental shocks, the market fraction evolves closer to one steady state over time. However, a large shock can push the fraction into the basin of attraction of the other steady state. Therefore, switching occurs with occasional large shocks. The "switch size" depends on the difference between the two steady state levels. A larger difference leads to more significant switching among the population. As b increases to $b = 20$ in Fig. 3 (b) and then $b = 100$ in Fig. 3 (c), switching becomes more frequent.

We can further measure the dependence of switching intensity on parameter b. To measure the switching intensity, we first define a *switch* as follows. Suppose that m_t is in one of its steady states at time t_0, e.g., $m_{t_0} = m^*_+$. The earliest time at which m_t, $t > t_0$ can reach the other steady state is denoted as t_1, i.e., $m_{t_1} = m^*_-$. The earliest time after t_1 when m_t can switch back to the steady state (at time t_0) is denoted as t_2, i.e., $m_{t_2} = m^*_+$. Similarly, we denote t_3 as the nearest time when m_t switches to m^*_-, $\cdots$, and t_N as the time of the Nth switching. As a result, we obtain a time-series of switch times, for which the number of switches per unit of time is given by $N/(t_N - t_1)$. We then define the switching intensity of the mean choice as the average number of switches per unit of time based on Monte Carlo simulations. Based on 1,000 simulations, Fig. 3 (d) reports the switching intensity against b. It shows that the switching intensity increases with b.

Therefore, social interaction plays an important role in the choice dynamics in the population, leading to the existence of multiple mean choice regimes, and private utility shocks affect the persistence and switching intensity between the two regimes. The following section shows that the combination of persistent switching between different regimes provides an underlying mechanism of the two important stylized facts characterizing equilibrium asset returns in equity markets, namely, *volatility clustering* and *time-series momentum.*

4. Volatility Clustering

This section first establishes the connection between the two mean choice regimes and the two volatility regimes and then explores the impact on volatility dynamics. We show that social interaction is the underlying mechanism driving volatility switches between the two regimes, which leads to volatility clustering.

4.1. **Volatility Regimes.**

Corresponding to the stable steady states of the mean choice in (32), the conditional variance, $\sigma_t^2 = (V_{D,t})^2 + (V_{s,t})^2$, can have different regimes, depending on social interaction βJ.

Corollary 4.1. *(Volatility Regimes) For $b = 0$, corresponding to each stable steady state of the mean choice, we have the following volatility regimes:*

(i). *for $\beta J \leq 1$, there is a unique volatility regime*

$$\sigma_0^2 = \left[\frac{\sigma_D}{r} + \frac{\gamma_A + \gamma_B}{2r(r+\lambda)\sigma_D}\right]^2 + \left[\frac{\rho\sigma_f}{r(r+\lambda)}\right]^2 \quad \textit{for } m_0^* = 0; \tag{33}$$

(ii). *for $\beta J > 1$, there are two volatility regimes*

$$\sigma_+^2 = \left[\frac{\sigma_D}{r} + \frac{1}{r(r+\lambda)\sigma_D}\left(\frac{1+m^*}{2}\gamma_A + \frac{1-m^*}{2}\gamma_B\right)\right]^2 + \left[\frac{\sigma_f\rho(1+m^*\epsilon)}{r(r+\lambda)}\right]^2 \quad \textit{for } m_+^* = m^* > 0; \tag{34}$$

$$\sigma_-^2 = \left[\frac{\sigma_D}{r} + \frac{1}{r(r+\lambda)\sigma_D}\left(\frac{1-m^*}{2}\gamma_A + \frac{1+m^*}{2}\gamma_B\right)\right]^2 + \left[\frac{\sigma_f\rho(1-m^*\epsilon)}{r(r+\lambda)}\right]^2 \quad \textit{for } m_-^* = -m^* < 0, \tag{35}$$

where

$$\sigma_-^2 - \sigma_+^2 = \frac{8rm^*\rho^2\epsilon[\sigma_f/(r(r+\lambda))]^2}{\sqrt{\lambda^2 + [1-\rho^2(1+\epsilon)^2]\sigma_f^2/\sigma_D^2} + \sqrt{\lambda^2 + [1-\rho^2(1-\epsilon)^2]\sigma_f^2/\sigma_D^2}} > 0. \tag{36}$$

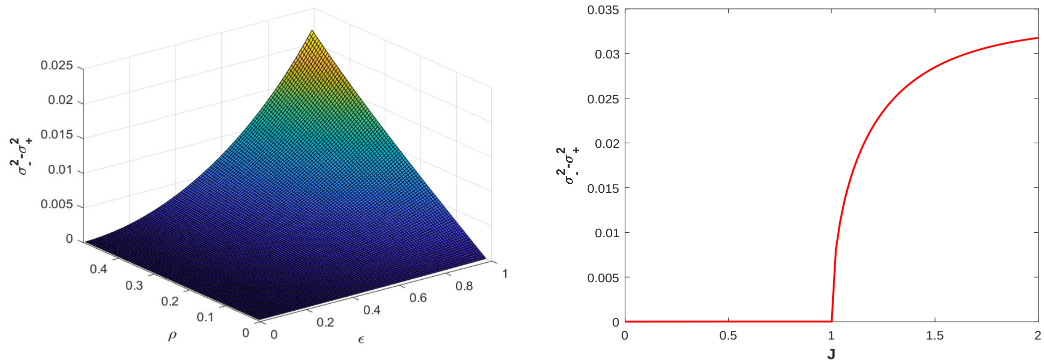

FIGURE 4. Dependence of the difference in volatility between two regimes, $\sigma_-^2 - \sigma_+^2$, on (a) ρ and ϵ and (b) J. The parameters are given by Table 1.

Intuitively, the equilibrium mean choice affects return volatility. Corollary 4.1 implies that with strong social interaction, there is a low-volatility regime corresponding to $m_+^* > 0$, where the majority of investors choose to believe that the public signal is relatively more informative. Thus, the aggregate market perceives less uncertainty, and asset returns become less volatile. On the other hand, there is a high-volatility regime corresponding to $m_-^* < 0$, where the majority of investors choose to believe that the public signal is relatively less informative. In particular, conditional volatility is the highest when all investors choose to believe that the public signal is pure noise (i.e., $\phi_t = 0$ and $\rho_B \equiv \rho(1-\epsilon) = 0$) with

$$\sigma_t = \sigma_{max} := \frac{\sigma_D}{r}\left(1 + \frac{1}{r+\lambda}\left[\sqrt{\lambda^2 + \frac{\sigma_f^2}{\sigma_D^2}} - \lambda\right]\right) \tag{37}$$

and the lowest when all investors choose to believe that the public signal is perfectly informative (i.e., $\phi_t = 1$ and $\rho_A \equiv \rho(1+\epsilon) = 1$) with

$$\sigma_t = \sigma_{min} := \frac{\sigma_f}{r(r+\lambda)}. \tag{38}$$

Moreover, the difference in volatility, $\sigma_-^2 - \sigma_+^2$, between the two regimes, m_-^* and m_+^*, in (36) increases in signal informativeness (ρ), dispersion of beliefs about this informativeness (ϵ), and social interactions (J), which is illustrated in Fig. 4.[19] This is because strong social interaction leads to a more polarized mean choice, which, coupled with large dispersion in beliefs about signal informativeness, results in a greater difference in volatility between the two regimes.

4.2. **Time-Series Simulation.** To better understand the underlying mechanism for regime switching and volatility clustering, we first perform time-series simulations to explore some properties of the full model. With strong social interaction ($J = 1.15$), based on a typical simulation, Fig. 5 illustrates time-series of (a) asset price P_t (red solid line) and benchmark price P_t^* when every investor believes the true ρ (blue dotted line), (b) asset returns dP_t (in price changes), (c) mean choice and hence the population fraction ϕ_t, and (d) private utility h_t.[20] From Fig. 5, we have three observations.

First, the equilibrium price P_t fluctuates around the benchmark fundamental price P_t^* in general but can sometimes differ significantly, as illustrated in Fig. 5 (a). This demonstrates the effect of information uncertainty and different interpretations of signal informativeness on the asset price, with the mean-preserved spread in the informativeness not canceling out in equilibrium. However, does it cancel out on average? By comparing the equilibrium price with the benchmark price, we have

$$P_t - P_t^* = \frac{1}{r(r+\lambda)}\left[\phi_t(\hat{f}_t^A - \hat{f}_t^*) + (1-\phi_t)(\hat{f}_t^B - \hat{f}_t^*)\right]. \tag{39}$$

It can be verified that based on the dividend dynamics in (1) and (2), the unconditional expectation $\mathbb{E}[\hat{f}_t^k - \hat{f}_t^*] = 0$ ($k = A, B$). Therefore, when the mean choice stays constant, the equilibrium and benchmark prices converge in expectation. However, this is no longer true when the mean choice is time varying, driven by both the private and social utility components.

[19]Due to rescaling, we fix $\beta = 1$ in our discussion.

[20]We report the simulation results for the last $5,000$ periods (approximately 20 years) after a burn-in period of $25,000$ (approximately 100 years) to ensure that the distribution of the population fraction ϕ_t is stationary.

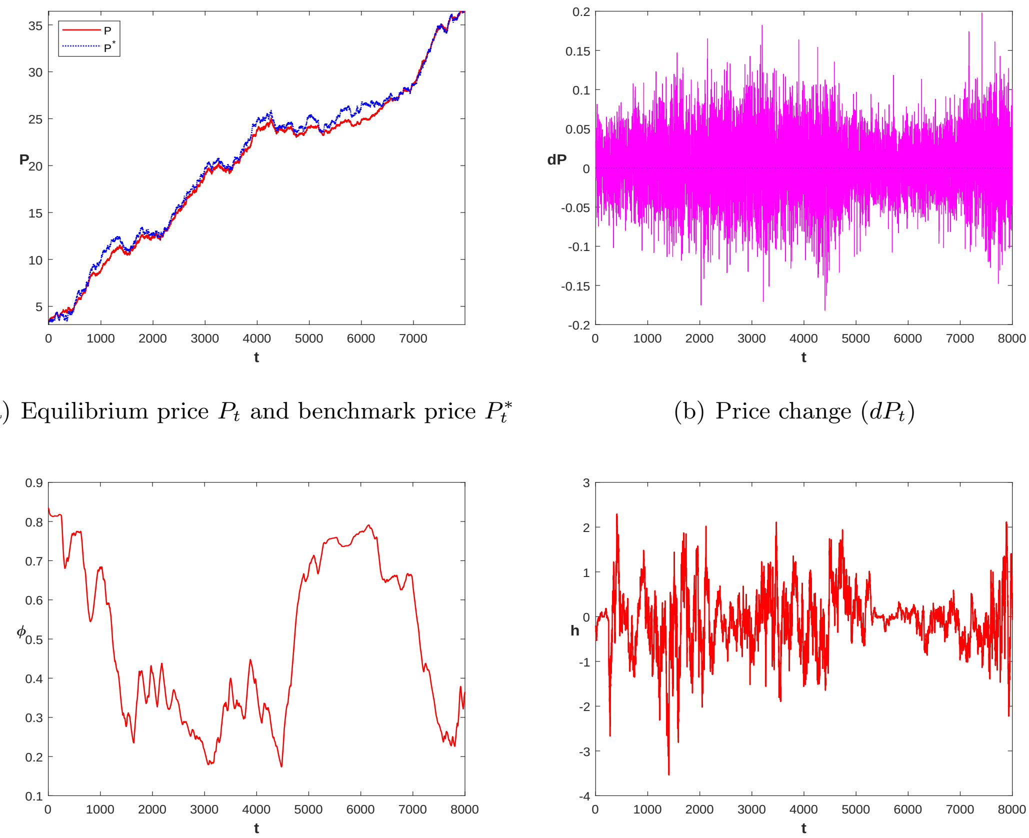

(a) Equilibrium price P_t and benchmark price P_t^*

(b) Price change (dP_t)

(c) Population fraction ϕ_t

(d) Private value h_t

FIGURE 5. Time series of (a) the asset price (red solid line) and the fundamental price (blue dotted line), (b) the asset returns, (c) the population fraction and (d) the private value; the rest of the parameters are given in Table 1.

Second, Figs. 5 (b) and (c) show that both the population and return volatility are time varying and persistent in each regime but can switch between the two regimes (explored in Section 3). Correspondingly, asset returns exhibit persistent volatility in both of the two volatility regimes, while switching regimes from time to time. More explicitly, ϕ_t does not settle into either one of the two regimes in the long run (even after a burn-in period of approximately 100 years), and returns are more (less) volatile when the mean choice is low (high). This is consistent with Corollary 4.1 and further demonstrated by the negative correlation $Corr[(dP_t)^2, \phi_t] = -0.24$.

Third, Fig. 5 (d) shows that private utility h_t fluctuates around zero with occasionally (positive or negative) large spikes. Intuitively, these occasional but large spikes in h_t are driven by large dividend and public signal shocks, which can potentially trigger switching of the mean choice between the low and high regimes. This is further demonstrated by the fact that h_t and ϕ_t are weakly and positively correlated with $Corr[h_t, \phi_t] = 0.08$.

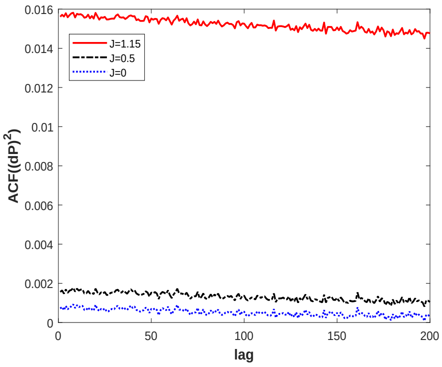

(a) Daily volatility ACFs for J=0.5 and 1.15

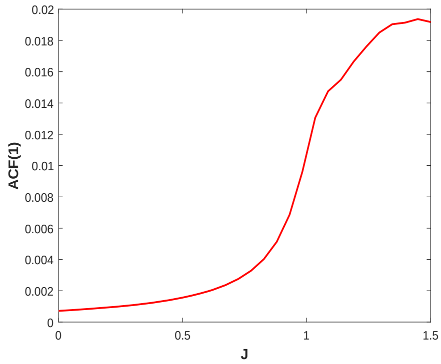

(b) Monthly volatility ACF(1)

FIGURE 6. Average autocorrelation functions (ACFs) of (a) daily volatility $(dP)^2$ with $J = 0.5, 1.15$ over 200 days and (b) first-order monthly volatility $(dP)^2$, ACF(1), with respect to J; the other parameters are given by Table 1.

4.3. **Volatility Autocorrelation and Clustering.** Fig. 6 (a) shows the autocorrelation pattern for the simulated daily squared returns for up to 200 lags.[21] First, if we use squared returns as a measure of volatility, current volatility is most affected by the most recent return shock, and then the effect decays over longer lags at a very slow rate; i.e., volatility is highly persistent. This autocorrelation pattern of volatility is commonly observed in equity market indices. Furthermore, we also observe that the autocorrelation at the first lag, i.e., ACF(1), is higher for larger values of J. This is further demonstrated in Fig. 6 (b), where we plot the monthly ACF(1) against values of J, which shows that stronger social interaction can significantly increase ACF(1), i.e., the impact of the return shock in the previous month on the return volatility in the current month. The autocorrelation pattern of volatility with respect to social interaction leads to the following observation on volatility clustering, together with the underlying mechanism and intuition.

With social interaction, investors have incentives to conform to the mean choice of the population. According to Proposition 2.1, the volatility coefficients, $V_{D,t}$ and $V_{s,t}$, are linear functions of the mean choice (via the market fraction, ϕ_t). Supposing that the mean

[21]The results are based on 1,000 simulations. Without social interaction, the time variation in the mean choice becomes minimal; as a result, the ACFs become insignificant.

choice is a constant, past returns would have no impact on volatility, which would stay constant. Therefore, the impact of past returns on current volatility is directly affected by the mean choice.

When social interaction is weak, m_0^* is the unique steady state for the mean choice. This corresponds to the unique volatility regime σ_0^2. Past returns, which translate to private utility shocks, may cause the mean choice to fluctuate. Because of the global stability of m_0^*, the mean choice tends to revert back to the steady state, so the impact of past returns on current volatility is relatively weak. Therefore, the effect of past return shocks is mitigated, and volatility is less persistent.

However, when social interaction is strong, investors have more incentives to conform to the mean choice of the population. This leads to two additional steady states for the mean choice, $m_-^* < 0$ and $m_+^* > 0$. They correspond to two volatility regimes, a high regime σ_+^2 and a low regime σ_-^2. Channeled by private utility shocks, past returns can have a much larger impact on the current mean choice and hence volatility. Because of the local stability of the mean choice steady states, m_-^* and m_+^*, private utility shocks (from past returns) can have two effects. First, occasionally large shocks can potentially lead volatility to switch between the high- and low-volatility regimes, which amplifies the effect of past return shocks on current volatility. Second, with small shocks most of the time, volatility becomes more persistent in either the high- or the low-volatility regime (due to local stability). Therefore, with strong social interaction, volatility becomes more persistent and clustered; high volatility tends to be followed by high volatility, and low volatility tends to be followed by low volatility, as illustrated in Fig. 5 (b).

4.4. **Excess Volatility.** We also show that strong social interaction can lead to *excess volatility*; i.e., price volatility, measured by the standard deviation of price changes, can exceed the level in the benchmark case.[22] Particularly, price volatility is affected by fluctuations in $\hat{f}_t^i$ and hence the mean choice. When $\beta J > 1$, due to the persistence of multiple steady states, the mean choice can experience large swings over time between the two regimes; thus, price volatility increases. Additionally, price volatility decreases in true informativeness ρ. As ρ decreases, the public signal becomes less informative about the fundamental, which increases price volatility. Furthermore, when social interaction is strong, a larger dispersion in informativeness makes prices more volatile.

[22]See Appendix B for details.

5. Time-Series Momentum

Moskowitz et al. (2012) investigate time-series momentum, that is, the strong positive predictive ability of a security's own past returns at monthly level. Zhou and Zhu (2014) demonstrate that the risk-sharing function provided by trend-following trading rules gives rise to positive autocovariance of returns. In examining autocovariance of asset returns, we posit social interaction as an alternative channel for the momentum observed in the time-series of equity index returns.

The autocovariance of asset returns under the objective probability measure $\mathbb{P}^*$ is defined as $\langle P_t - P_{t-\tau}, P_{t+\tau} - P_t\rangle$, where t and τ are at the monthly level.[23] We first examine the benchmark model without information uncertainty. The autocovariance of the fundamental asset returns is characterized by the following proposition.

Proposition 5.1. *The autocovariance of asset returns in the benchmark without information uncertainty is given by*

$$\begin{aligned}\langle P_t^* - P_{t-\tau}^*, P_{t+\tau}^* - P_t^*\rangle = &-\frac{\gamma}{r\lambda^2}\Big(\frac{1}{r} - \frac{1}{r+\lambda}\Big)(1-e^{-\lambda\tau})^2 \\ &- \frac{1}{2\lambda^3}\Big(\frac{1}{r} - \frac{1}{r+\lambda}\Big)^2\Big(\frac{\gamma^2}{\sigma_D^2} + \rho^2\sigma_f^2\Big)(1-e^{-\lambda\tau})^2\big(1+e^{-\lambda(2t-\tau)}\big).\end{aligned} \tag{40}$$

Proposition 5.1 shows that the autocovariance is *negative* for the benchmark case. This is due to the fact that the stochastic trend f_t is a mean-reverting process. Next, we examine return autocovariance in the case with information uncertainty and social interaction.

Proposition 5.2. *The autocovariance of the asset returns in the full model with social interactions is given by*

$$\langle P_t - P_{t-\tau}, P_{t+\tau} - P_t\rangle = \frac{1}{r\lambda^2}\Big(\frac{1}{r} - \frac{1}{r+\lambda}\Big)\Phi + \frac{1}{2\lambda^3}\Big(\frac{1}{r} - \frac{1}{r+\lambda}\Big)^2\Big(\frac{1}{\sigma_D^2}\Psi_1\Psi_2 + \sigma_f^2\Psi_3\Psi_4\Big), \tag{41}$$

where Φ, Ψ_1, Ψ_2, Ψ_3 and Ψ_4 are given in Appendix A.2. In particular, when the population fraction is fixed, for example, $\phi_t = \bar{\phi}$,

$$\begin{aligned}\langle P_t - P_{t-\tau}, P_{t+\tau} - P_t\rangle = &-\frac{1}{r\lambda^2}\Big(\frac{1}{r} - \frac{1}{r+\lambda}\Big)(1-e^{-\lambda\tau})^2[\bar{\phi}\gamma_A + (1-\bar{\phi})\gamma_B] \\ &- \frac{1}{2\lambda^3}\Big(\frac{1}{r} - \frac{1}{r+\lambda}\Big)^2\Big\{\frac{1}{\sigma_D^2}[\bar{\phi}\gamma_A + (1-\bar{\phi})\gamma_B]^2 \\ &+ \sigma_f^2\rho^2[1+\epsilon(2\phi_t - 1)]^2\Big\}(1-e^{-\lambda\tau})^2\big(1+e^{-\lambda(2t-\tau)}\big).\end{aligned} \tag{42}$$

[23]We study the case with the same lookback period and holding period for parsimony. In general, they can be different in the empirical literature.

Proposition 5.2 shows that the autocovariance of asset returns can be either positive or negative over time due to social interaction. Particularly, without social interaction, the market fraction is constant, and asset returns are always negatively correlated.

When the mean choice is time varying, it can be shown (see Appendix A.2) that when $(\phi_{t+\tau} - \phi_t)(\phi_t - \phi_{t-\tau}) > 0$, the autocovariance is positive over small time horizons. This observation implies that social interaction can lead to momentum (in the sense of positive return autocovariance) when the mean choice is persistent. Intuitively, when one choice is made by the majority of investors, it becomes more attractive for individual investors. As a result, they pull the price closer to their valuation. In particular, when the mean choice is persistent over a short time horizon, the market price maintains a price trend driven by the dominant group of investors, resulting in time-series momentum in the short run.

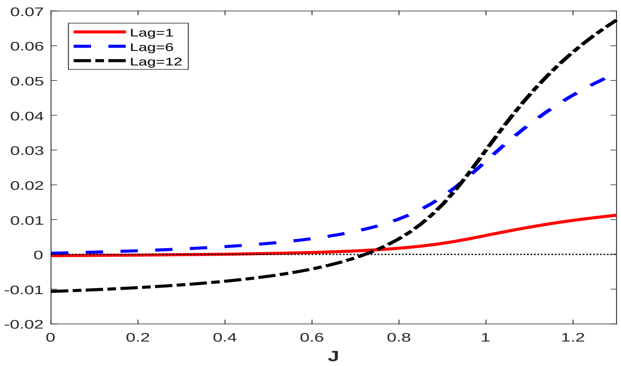

(a)

FIGURE 7. Estimated slope coefficient from the regression of next month's return onto a constant and past average returns over lookback periods of 1, 6, and 12 months using the model-generated data with parameters given by Table 1.

We further conduct a numerical analysis to verify the above theoretical results and intuitions. Fig. 7 reports the average slope coefficient from the regression of next month's return onto past average returns over $\tau = 1, 6$ and 12 month lookback periods.[24] It shows that the coefficient is increasing in J, becoming more significant with a longer lookback period. Intuitively, with weak social interaction, the mean choice tends to converge to

[24]We numerically simulate the system based on daily parameters and convert the daily returns to monthly returns (21 days a month). Then, we run the following regression using the monthly returns: $r_t = a + b\frac{1}{\tau}\sum_{s=1}^{\tau} r_{t-s} + \varepsilon$. Fig. 7 plots the average slope coefficient based on 1,000 simulations against social interactions J.

the only stable steady state, leading to a small or negative monthly coefficient. However, with strong social interaction, the short-term persistence of the mean choice in each regime tends to generate a significantly positive coefficient, which leads to price momentum in the short run. This is consistent with the findings in the literature, e.g., in Fama and French (1988), Poterba and Summers (1988), Culter, Poterba and Summers (1991), and He and Li (2015*a*). The results are also consistent with the above analysis. In fact, over a short period such as one month, ϕ_t (or m_t) is governed by the ODE in (22), whose solutions fluctuate between 0 and 1 gradually and smoothly.[25] When switching intensity is low (less than once a month), it is more likely that $(\phi_{t+\tau}-\phi_t)(\phi_t-\phi_{t-\tau}) > 0$ holds for the simulated sample path, which generates positive autocorrelation and hence momentum in the short run.

6. Empirical Analysis

In this section, we provide an empirical validation of our theoretical model predictions, namely, that volatility clustering and time-series momentum are more prominent under strong than under weak social interaction. We propose using StockTwits (`stocktwits.com`) post volume as a measure of social interaction.[26] Intuitively, a high post volume tends to reflect high social interaction. StockTwits and Twitter data have recently been used in the literature to measure investor sentiment (Oliveira et al., 2013; Agrawal et al., 2018; Cookson and Niessner, 2020) and disagreement and attention (Sprenger et al., 2014) and to study their effects on stock market variables, such as returns, volatility, and liquidity (Antweiler and Frank, 2004; Oliveira et al., 2013; Chen et al., 2014; and Li et al., 2016).

6.1. **Data.** We use daily data for five market indices (S&P 500, Nasdaq Composite index, NYSE Composite index, Dow Jones Industrial Average, and Wilshire 5000) from 1 January 2010 to 30 September 2019. Closing daily price data are from Thomson Reuters Datastream. As mentioned above, we use the number of daily posts on StockTwits as a measure of social interaction. Our data on the daily number of posts exchanged on StockTwits cover the same period.

[25]In particular, when $h_t = 0$, ϕ_t (or m_t) is governed by a one-dimensional ODE whose solutions are monotonic. In this case, the condition $(\phi_{t+\tau} - \phi_t)(\phi_t - \phi_{t-\tau}) > 0$ always holds for small τ.

[26]StockTwits is an online financial platform with a total monthly audience of approximately 1.5 million users, with 60% of its users under 44. Like Twitter tweets, StockTwit messages are of a small size (maximum 140 characters) and consist of ideas, links, charts and other data. However StockTwits is exclusively about investing.

Given that the number of StockTwits users has increased exponentially since 2010 together with the volatility of the daily number of posts exchanged on the platform, we first perform a log-transformation to eliminate heteroskedasticity in the data and then detrend.[27] Fig. 8 shows the transformed social interaction series, which is referred to as $Inter_t$.

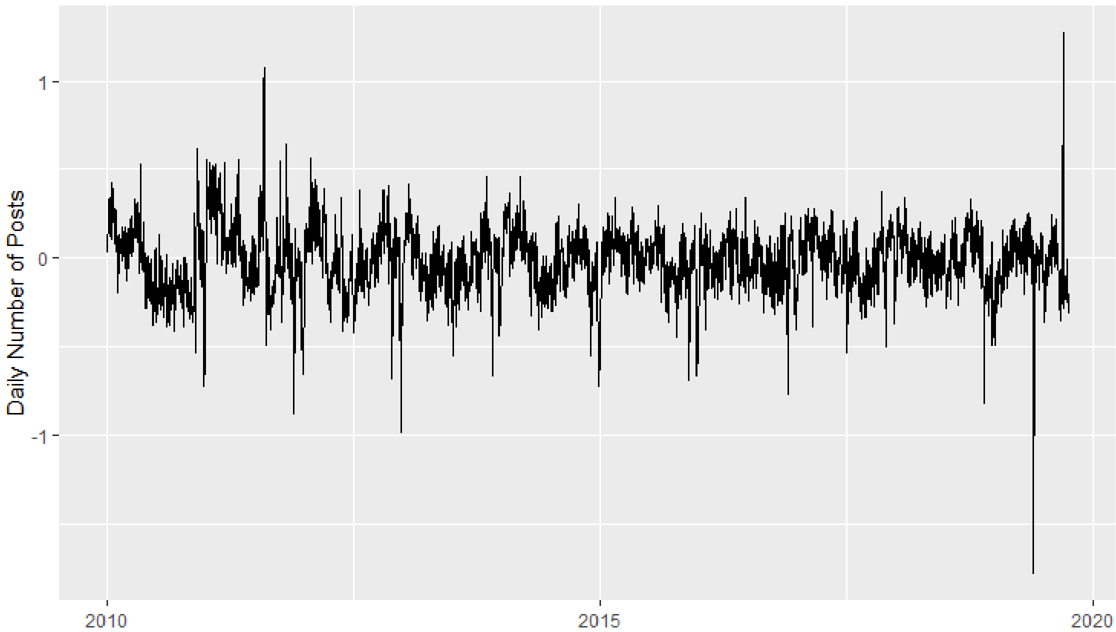

FIGURE 8. Transformed social interaction time series ($Inter$) after log transformation and removal of the trend from the time series of the daily number of posts exchanged on StockTwits.

Since several stationarity tests confirm the stationarity of the transformed social interaction series,[28] we use a unique threshold for the entire sample period to identify days with strong/weak social interaction. Specifically, we use the top 30% of daily social interaction to identify days with strong social interaction and the bottom 30% to identify days with weak social interaction. The dichotomous variable for strong social interaction (SI_{strong}) is equal to one on day t when social interaction on day t is greater than the 70th percentile of daily social interaction and zero otherwise. Similarly, the dichotomous variable for weak

[27]We use the time-series decomposition by Loess proposed in Cleveland at al. (1990) to remove the trend component.

[28]These tests include the Kwiatkowski-Phillips-Schmidt-Shin test, the Phillips-Perron unit root test, and the augmented Dickey-Fuller test.

social interaction (SI_{weak}) is equal to one on day t if social interaction on day t is less than the 30th percentile of daily social interaction and zero otherwise.[29]

In what follows, we use squared returns and the GARCH model to study the relationship between social interaction and volatility. Squared returns measure historical volatility. Fig. 9 shows the cross-correlation function of volatility at time t, measured by squared returns, with social interaction at time $t-k$. We can observe that for all the market indices, volatility is significantly positively correlated with social interaction on the same day and at 1 and 2 day lags. This implies that social interaction has a positive and significant impact on current and future volatility up to two days ahead.

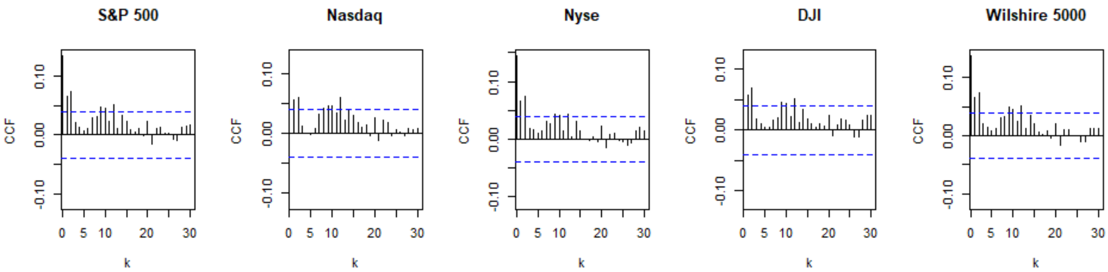

FIGURE 9. Cross-correlation function (CCF) between $Inter_{t-k}$ and Vol_t, measured by the correlation between volatility (in squared returns) and lagged social interaction.

6.2. **Regression Analysis on Squared Returns.** In this subsection, we examine the impact of social interaction on the serial correlation of squared returns for equity indices by using the detrended time series $Inter$ and consider its interaction with the lagged squared returns. More specifically, we run the following regression by ordinary least squares (OLS),

$$log(1+Vol_t) = \alpha + \beta_1 log(1+Vol_{t-1}) + \beta_2 Inter_t \times log(1+Vol_{t-1}) + \epsilon_t, \qquad (43)$$

where Vol_t is the volatility, measured by squared returns, on day t and $Inter_t$ is the transformed social interaction on day t. In (43), we are interested in the sign of the β_2 coefficient. Specifically, a positive and significant β_2 coefficient would imply that the serial correlation in squared returns increases with social interaction.

Table 2 reports the OLS estimates of Eq. (43) for 5 equity indices. It shows that consistently across all the indices, β_2 is positive and highly significant. This finding confirms the model prediction that volatility clustering is more prominent with stronger social interaction since squared returns are more serially correlated when the proxy is high.

[29]We also conduct the analysis with alternative percentile thresholds for daily social interaction, and the results are qualitatively the same.

	S&P 500	Nasdaq	NYSE	DJIA	Wilshire 5000
Constant	0.723***	0.992***	0.779***	0.636***	0.758***
	(0.100)	(0.117)	(0.125)	(0.078)	(0.108)
$log(1 + Vol_{t-1})$	0.172***	0.149***	0.141***	0.196***	0.164***
	(0.035)	(0.026)	(0.029)	(0.044)	(0.032)
$Inter_t \times log(1 + Vol_{t-1})$	0.282***	0.332***	0.305***	0.284***	0.285***
	(0.055)	(0.041)	(0.042)	(0.084)	(0.048)
R^2	0.077	0.069	0.076	0.077	0.079
Adjusted R^2	0.077	0.068	0.076	0.076	0.078

$^{***}p < 0.01$, $^{**}p < 0.05$,$^{*}p < 0.1$

TABLE 2. Volatility and social interaction (continuous variable) – The table reports the OLS estimates of the model in Eq. (43), where Newey-West standard errors are reported in parentheses. The constant term is reported in basis points.

To explore the effect of weak and strong social interaction, we run the following regression:

$$\begin{aligned} log(1 + Vol_t) =& \alpha + \beta log(1 + Vol_{t-1}) + \beta_s SI_{strong,t} \times log(1 + Vol_{t-1}) + \\ & \beta_w SI_{weak,t} \times log(1 + Vol_{t-1}) + \epsilon_t. \end{aligned} \tag{44}$$

We include the interaction terms of lagged squared returns with the dichotomous variables for strong and weak social interactions, $SI_{strong} \times \log(1 + Vol_{t-1})$ and $SI_{weak} \times \log(1 + Vol_{t-1})$, respectively. A positive (negative) and significant β_s (β_w) coefficient would imply that the serial correlation in squared returns is higher (lower) when social interaction is stronger (weaker) than when it is at normal levels (between the 30th and 70th percentiles). This is confirmed by the results in Table 3, though β_w is not statistically significant. Again, these results are very much in line with the model prediction.

6.3. **GARCH Analysis.** The GARCH model is commonly employed in modeling financial time series that exhibit time-varying volatility and volatility clustering. In this section, we explore the relationship between social interaction and volatility clustering by

	S&P 500	Nasdaq	NYSE	DJIA	Wilshire 5000
Constant	0.711***	0.964***	0.761***	0.633***	0.744***
	(0.080)	(0.090)	(0.117)	(0.051)	(0.093)
$log(1 + Vol_{t-1})$	0.116***	0.112***	0.076***	0.119***	0.105***
	(0.040)	(0.031)	(0.029)	(0.041)	(0.037)
$SI_{strong,t} \times log(1 + Vol_{t-1})$	0.302***	0.279***	0.331***	0.298***	0.309***
	(0.069)	(0.074)	(0.056)	(0.090)	(0.061)
$SI_{weak,t} \times log(1 + Vol_{t-1})$	−0.032	−0.036	−0.011	−0.005	−0.022
	(0.056)	(0.040)	(0.033)	(0.064)	(0.050)
R^2	0.088	0.071	0.085	0.088	0.088
Adjusted R^2	0.087	0.069	0.084	0.087	0.087

$^{***}p < 0.01$, $^{**}p < 0.05$, $^{*}p < 0.1$

TABLE 3. Volatility and social interaction (dichotomous variables) – The table reports the OLS estimates of the model in Eq. (44), where Newey-West standard errors are reported in parentheses. The constant term is reported in basis points.

estimating the following GARCH(1,1) model:[30]

$$\begin{aligned}
r_t =& \gamma + \epsilon_t \\
\epsilon_t =& \eta_t \sqrt{\nu_t}, \quad \eta \sim N(0,1) \\
\nu_t =& \omega_n + \alpha_n \epsilon_{t-1}^2 + \beta_n \nu_{t-1} + SI_{strong,t}\omega_s + SI_{strong,t}\alpha_s \epsilon_{t-1}^2 + SI_{strong,t}\beta_s \nu_{t-1} + \\
& SI_{weak,t}\omega_w + SI_{weak,t}\alpha_w \epsilon_{t-1}^2 + SI_{weak,t}\beta_w \nu_{t-1},
\end{aligned} \tag{45}$$

where r_t is the return on day t, η is white noise with zero mean and unit standard deviation, ν_t is the variance on day t, and SI_{strong} (SI_{weak}) equals one when social interaction is strong (weak) and zero otherwise. To guarantee that ν_t is positive, we impose the following conditions: $\omega_n > 0$, $\alpha_n \geq 0$, $\beta_n \geq 0$, $\omega_n + \omega_s > 0$, $\alpha_n + \alpha_s \geq 0$, and $\beta_n + \beta_s \geq 0$, $\omega_n + \omega_w > 0$, $\alpha_n + \alpha_w \geq 0$, and $\beta_n + \beta_w \geq 0$. We also impose the stationarity conditions $\alpha_n + \beta_n < 1$, $\alpha_n + \alpha_s + \beta_n + \beta_s < 1$, and $\alpha_n + \alpha_w + \beta_n + \beta_w < 1$.

In the GARCH model, volatility depends on all past shocks to volatility. In fact, consider a standard GARCH(1,1) model, $\nu_t = \omega + \alpha\epsilon_{t-1}^2 + \beta\nu_{t-1}$, which can be written in the following form:

$$\nu_t = \frac{\omega}{1-\beta} + \alpha\epsilon_{t-1}^2 + \alpha\sum_{s=1}^{\infty}\beta^s\epsilon_{t-s-1}^2. \tag{46}$$

[30]The GARCH(1,1) model is selected based on the Akaike information criterion by comparing different orders of the GARCH model.

	S&P 500	Nasdaq	NYSE	DJIA	Wilshire 5000
α_n	0.143***	0.115***	0.120***	0.146***	0.131***
	(0.018)	(0.015)	(0.016)	(0.018)	(0.017)
α_s	0.083***	0.086***	0.090***	0.089***	0.078***
	(0.028)	(0.026)	(0.026)	(0.029)	(0.026)
α_w	−0.049**	−0.048***	−0.010	−0.055***	−0.039**
	(0.022)	(0.020)	(0.021)	(0.022)	(0.021)
β_n	0.785***	0.819***	0.805***	0.7867***	0.792***
	(0.022)	(0.020)	(0.022)	(0.022)	(0.022)
β_s	−0.016	−0.049	−0.016	−0.023	−0.003***
	(0.042)	(0.043)	(0.041)	(0.043)	(0.042)
β_w	0.102***	0.076***	0.081***	0.097***	0.096***
	(0.031)	(0.031)	(0.032)	(0.033)	(0.031)
γ	0.001***	0.001***	0.001***	0.001***	0.001***
	(0.000)	(0.000)	(0.000)	(0.000)	(0.000)
ω_n	0.028***	0.034***	0.025***	0.025***	0.031***
	(0.008)	(0.012)	(0.008)	(0.008)	(0.008)
ω_s	0.030**	0.060**	0.024*	0.025*	0.024*
	(0.016)	(0.028)	(0.016)	(0.016)	(0.016)
ω_w	-0.011	0.004	-0.014	-0.009	-0.014
	(0.015)	(0.024)	(0.016)	(0.014)	(0.016)

$^{***}p < 0.01$, $^{**}p < 0.05$, $^{*}p < 0.1$

TABLE 4. Maximum likelihood estimates of GARCH(1,1) and social interaction (dichotomous variable) model (45), with standard errors in parentheses. Omega parameters are reported in basis points.

Here, α measures the impact of the initial return shock on current volatility, and β measures the persistence rate. Our model predicts that social interaction should increase α but not necessarily β, which is exactly what we see in the results reported in Table 4.

Table 4 reports the maximum likelihood estimates of the above GARCH(1,1) model. We observe that strong social interaction increases the impact of the initial return shock by 7.8 to 9%, whereas weak social interaction reduces the impact by 3.9 to 5.5% (except for the NYSE); both of these effects are highly significant. The persistence rate β tends to increase under weak social interaction and decrease under strong social interaction, although the latter effect is not statistically significant.

In summary, the empirical results reported in Tables 3 and 4 lend support to our model prediction about the relationship between volatility and social interaction. Both theory and empirical evidence show that the effect of volatility clustering intensifies during periods of strong social interaction and fades during periods of weak social interaction.

6.4. **Time-Series Momentum.** Time-series momentum implies that the past 12 month excess return of an equity index is a positive predictor of its future return. To investigate the relationship between social interaction and time-series momentum, we study the profitability of time-series momentum strategies in the two social interaction regimes. A time-series momentum strategy longs the index if the excess return over the past k months is positive and shorts the index if the excess return over the past k months is negative. Thus, for asset i, the return of the time-series momentum strategy with a k month look-back period and a one month holding period is given by the following formula (Moskowitz et al., 2012):

$$r_{t,t+1}^{TSM(k),i} = sign(r_{t-k,t}^{i})r_{t,t+1}^{i}, \tag{47}$$

where $r_{t-k,t}^{i}$ is the excess return of asset i from $t-k$ to t. The function $sign(\cdot)$ gives 1 when its argument is positive and -1 when its argument is negative. We estimate the time-series momentum returns by controlling for the Carhart four factors (Carhart, 1997),

$$r_t^{TSM(k),i} = \alpha_n + \alpha_s SI_{strong,t} + \alpha_w SI_{weak,t} + \beta_1 MKT_t + \beta_2 SMB_t + \beta_3 HML_t + \beta_4 UMD_t + \epsilon_t, \tag{48}$$

where $SI_{strong,t}$ ($SI_{weak,t}$) equals one when more than 30% of the days in month t experience strong (weak) social interaction and zero otherwise. The risk-adjusted return of the time-series momentum strategy is given by α_n for neutral social interaction, by $\alpha_n + \alpha_s$ for strong social interaction and by $\alpha_n + \alpha_w$ for weak social interaction. Note that to be consistent with the time-series momentum literature, in this section, we use data at monthly frequency.

Table 5 reports the risk-adjusted returns (with Newey and West (1987) standard errors in parentheses) of the time-series momentum strategy – with controls for the Carhart four factors – for strong and weak social interactions, $\alpha_n+\alpha_s$ and $\alpha_n+\alpha_w$, respectively. It shows that the time-series momentum strategy reports higher alphas when social interaction is strong than when it is weak. Moreover, the risk-adjusted returns are always positive for strong social interaction and always negative for weak social interaction, although the alphas are not statistically significant in some cases. For example, the time-series momentum strategies on the S&P500 with a six month lookback period deliver an alpha of 1.27% per month during periods of strong social interaction and an alpha of -1.195% per month during periods of weak social interaction. Overall, the risk-adjusted returns

	Lookback period (months)					
	6		9		12	
Interaction	Strong	Weak	Strong	Weak	Strong	Weak
S&P 500	1.270***	−1.195*	0.775*	−1.333	0.678	−1.452
	(0.192)	(0.113)	(0.249)	(0.127)	(0.231)	(0.141)
Nasdaq	1.698***	−0.647	1.019**	−1.218	1.197***	−1.064
	(0.208)	(0.118)	(0.221)	(0.120)	(0.233)	(0.139)
NYSE	0.378	−1.389**	0.566	−0.857	0.178	−0.738
	(0.229)	(0.136)	(0.247)	(0.148)	(0.238)	(0.159)
DJIA	1.196**	−1.600**	0.667	−1.225	1.180**	−1.401*
	(0.180)	(0.099)	(0.231)	(0.120)	(0.194)	(0.122)
Wilshire 5000	1.256***	−0.642	0.776*	−1.403	0.603	−1.430
	(0.211)	(0.115)	(0.258)	(0.128)	(0.239)	(0.144)

$^{***}p < 0.01$, $^{**}p < 0.05$, $^{*}p < 0.1$

Table 5. Risk-adjusted returns of time-series momentum strategies in strong and weak social interactions (thresholds 30-40-30) with different lookback periods and a one month holding period and with the alphas (intercepts) for strong ($\alpha_n + \alpha_s$) and weak ($\alpha_n + \alpha_w$) social interaction from time-series regressions of (48) with lookback periods of 6, 9, and 12 months. Newey and West (1987) standard errors in parentheses. The alphas are expressed as a percentage.

are higher when social interaction is strong than when it is weak, which is true for all the indices with a 6 month lookback period, for three indices with a 9 month lookback period, and for two indices with a 12 month lookback period. These results are consistent with the model prediction that serial correlations in returns increase with social interaction and that returns tend to be positively (negatively) correlated when social interaction is strong (weak).

7. Conclusion

In this paper, we incorporate social interaction and information uncertainty into a random utility framework to develop a simple evolutionary equilibrium model of asset pricing and population dynamics. We show that social interaction influencing investors' belief choices can potentially provide a joint explanation for volatility clustering and short-run time-series momentum. As social interaction increases, investors' mean choice bifurcates from a unique stable steady state to two locally stable and asymmetric steady states, which leads to two volatility regimes. When social interaction is weak, shocks to private utility cause investors' mean choice and thus the population fractions corresponding to the different beliefs about signal informativeness to fluctuate around the unique steady state. The nonlinear interaction of these time-varying population fractions with the asset price then makes conditional volatility correlated and persistent. In contrast, when social interaction is strong, investors' mean choice switches between two steady states, leading to high- and low-volatility regimes, with volatility persistent in each regime. This type of constant switching between two persistent population fraction and volatility regimes can simultaneously generate mispricing, volatility clustering, and short-run time-series momentum.

Using StockTwits post volume as a proxy for social interaction for various equity indices, we further provide empirical evidence for our model predictions, showing autocorrelation in return volatility and the profitability of time-series momentum trading strategies driven by strong social interactions. The findings provide insights into the predictive power of time-varying investor population characteristics for returns.

References

Agrawal, S., Azar, P. D., Lo, A. W. and Singh, T. (2018), 'Momentum, mean-reversion, and social media: Evidence from stocktwits and twitter', *The Journal of Portfolio Management* **44**(7), 85–95.

Andersen, T. and Bollerslev, T. (1997), 'Heterogeneous information arrivals and return volatility dynamics: Uncovering the long-run in high frequency returns', *Journal of Finance* **52**(3), 975–1005.

Antweiler, W. and Frank, M. Z. (2004), 'Is all that talk just noise? the information content of internet stock message boards', *The Journal of Finance* **59**(3), 1259–1294.

Banerjee, A. (1992), 'A simple model of herd behavior', *Quarterly Journal of Economics* **107**, 797–817.

Barberis, N., Shleifer, A. and Vishny, R. (1998), 'A model of investor sentiment', *Journal of Financial Economics* **49**, 307–343.

Barucci, E. and Tolotti, M. (2012), 'Social interaction and conformism in a random utility model', *Journal of Economic Dynamics and Control* **36**, 1855–1866.

Becker, G. (1974), 'A theory of social interactions', *Journal of Political Economy* **82**(6), 1063–1093.

Bikhchandani, S., Hirshleifer, D. and Welch, I. (1992), 'A theory of fads, fashion, custom and cultural change as informational cascades', *Journal of Political Economy* **100**, 992–1026.

Blume, L. (2003), 'How noise matters', *Game and Economic Behavior* **44**, 251–271.

Blume, L. and Durlauf, S. (2003), 'Equilibrium concepts for social interaction models', *International Game Theory Review* **5**, 193–209.

Bollerslev, T. (1986), 'Generalized autoregressive conditional heteroskedasticity', *Journal of Econometrics* **31**, 307–327.

Brock, W. and Durlauf, S. (2001), 'Discrete choice with social interactions', *Review of Economic Studies* **68**, 235–260.

Brock, W. and Hommes, C. (1997*a*), *Models of Complexity in Economics and Finance*, Wiley, New York, pp. 3–44. in *Systems Dynamics in Economic and Finance Models*, Eds. Heij, C.and J.M. Schumacher and B. Hanzon and C. Praagman.

Brock, W. and Hommes, C. (1997*b*), 'A rational route to randomness', *Econometrica* **65**, 1059–1095.

Brock, W. and Hommes, C. (1998), 'Heterogeneous beliefs and routes to chaos in a simple asset pricing model', *Journal of Economic Dynamics and Control* **22**, 1235–1274.

Cao, H., Coval, J. and Hirshleifer, D. (2002), 'Sidelined investors, trading-generated news, and security returns', *Review of Financial Studies* **15**, 615–648.

Cao, H. and Ou-Yang, H. (2009), 'Differences of opinion of public information and speculative trading in stocks and options', *Review of Financial Studies* **22**, 299–335.

Carhart, M. (1997), 'On persistence in mutual fund performance', *Journal of Finance* **52**, 57—-82.

Chen, H., De, P., Hu, Y. J. and Hwang, B.-H. (2014), 'Wisdom of crowds: The value of stock opinions transmitted through social media', *The Review of Financial Studies* **27**(5), 1367–1403.

Chiarella, C., Dieci, R. and He, X. (2009), *Heterogeneity, Market Mechanisms and Asset Price Dynamics*, Elsevier, pp. 277–344. in *Handbook of Financial Markets: Dynamics and Evolution*, Eds. Hens, T. and K.R. Schenk-Hoppe.

Chiarella, C. and He, X. (2002), 'Heterogeneous beliefs, risk and learning in a simple asset pricing model', *Computational Economics* **19**, 95–132.

Cleveland, R., Cleveland, W., McRae, J. and Terpenning, I. (1990), 'STL: A seasonal-trend decomposition procedure based on loess', *Journal of Official Statistics* **6**(1), 3–73.

Cookson, J. A. and Niessner, M. (2020), 'Why don't we agree? evidence from a social network of investors', *The Journal of Finance* **75**(1), 173–228.

Culter, D., Poterba, J. and Summers, L. (1991), 'Speculative dynamics', *Review of Economic Studies* **58**, 529–546.

Daniel, K., Hirshleifer, D. and Subrahmanyam, A. (1998), 'Investor psychology and investor security market under-and overreactions', *Journal of Finance* **53**, 1839–1886.

Di Guilmi, C., He, X. and Li, K. (2014), 'Herding, trend chasing, and market volatility', *Journal of Economic Dynamics and Control* **48**, 349–373.

Dieci, R. and He, X.-Z. (2018), Heterogeneous agent models in finance, *in* 'Handbook of computational economics', Vol. 4, Elsevier, pp. 257–328.

Dumas, B., Kurshev, A. and Uppal, R. (2009), 'Equilibrium portfolio strategies in the presence of sentiment risk and excess volatility', *Journal of Finance* **64**, 195–229.

Engle, R. (1982), 'Autoregressive conditional heteroscedasticity with estimates of the variance of UK inflation', *Econometrica* **50**, 987–1008.

Engle, R. (2004), 'Risk and volatility: econometric models and financial practice', *The American Economic Review* **94**(3), 405–420.

Fama, E. and French, K. (1988), 'Permanent and temporary components of stock prices', *Journal of Political Economy* **96**, 246–273.

Feng, L. and Seasholes, M. (2004), 'Correlated trading and location', *Journal of Finance* **59**, 2117–2144.

Fleming, J., Kirby, C. and Ostdiek, B. (2006), 'Stochastic volatility, trading volume, and the daily flow of information', *The Journal of Business* **79**(3), 1551–1590.

Gaunersdorfer, A. and Hommes, C. (2007), *A Nonlinear Structural Model for Volatility Clustering*, Springer, Berlin/Heidelberge, pp. 265–288. in *Long Memory in Economics*, Eds. Teyssiere, G. and A. Kirman.

Hamilton, J. and Susmel, R. (1994), 'Autoregressive conditional heteroskedasticity and changes in regime', *Journal of Econometrics* **64**(1), 307–333.

Han, B. and Hirshleifer, D. (2012), 'Self-enhancing transmission bias and active investing', *working paper* .

He, X. and Li, K. (2012), 'Heterogeneous beliefs and adaptive behaviour in a continuous-time asset price model', *Journal of Economic Dynamics and Control* **36**, 973–987.

He, X. and Li, K. (2015*a*), 'Profitability of time series momentum', *Journal of Banking and Finance* **53**, 140–157.

He, X., Li, K. and Wang, C. (2016), 'Volatility clustering: A nonlinear theoretical approach', *Journal of Economic Behavior and Organization* **130**, 274–297.

He, X. and Li, Y. (2007), 'Power law behaviour, heterogeneity, and trend chasing', *Journal of Economic Dynamics and Control* **31**, 3396–3426.

He, X. and Li, Y. (2015*b*), 'Testing of a market fraction model and power-law behaviour in the DAX 30', *Journal of Empirical Finance* **31**, 1–17.

Heckman, J. (2001), 'Micro data, heterogeneity, and evaluation of public policy: Nobel lecture', *Journal of Political Economy* **109**, 673–748.

Heimer, R. (2016), 'Peer pressure: social interaction and the disposition effect', *Review of Financial Studies* **29**(11), 3177–3209.

Hommes, C. (2006), *Heterogeneous Agent Models in Economics and Finance*, Vol. 2 of *Handbook of Computational Economics*, North-Holland, pp. 1109–1186. in *Agent-based Computational Economics*, Eds. Tesfatsion, L. and K.L. Judd.

Hong, H., Kubik, J. and Stein, J. (2004), 'Social interactions and stock market participation', *Journal of Finance* **59**, 137–163.

Hong, H., Kubik, J. and Stein, J. (2005), 'Thy neighbor's portfolio: Word-of-mouth effects in the holdings and trades of money managers', *Journal of Finance* **60**, 2801–2824.

Hong, H. and Stein, J. (1999), 'A unified theory of underreaction, momentum trading, and overreaction in asset markets', *Journal of Finance* **54**, 2143–2184.

Ivković, Z. and Weisbenner, S. (2007), 'Information diffusion effects in individual investors' common stock purchases: Covet the neighbors' investment choices', *Review of Financial Studies* **20**, 1327–1357.

Jegadeesh, N. and Kim, W. (2010), 'Do analysts herd? An analysis of recommendations and market reactions', *Review of Financial Studies* **23**, 901–937.

Johnson, T. (2001), 'Return dynamics when persistence is unobservable', *Mathematical Finance* **11**(4), 415–445.

Kaustia, M. and Knüpfer, S. (2012), 'Peer performance and stock market entry', *Journal of Financial Economics* **104**, 321–338.

Keynes, J. (1936), *The general theory of employment, interest and money*, Harcourt, Brace and World, New York.

LeBaron, B. (2006), *Agent-based Computational Finance*, Vol. 2 of *Handbook of Computational Economics*, North-Holland, pp. 1187–1233. in *Agent-based Computational Economics*, Eds. Tesfatsion, L. and K.L. Judd.

Li, X., Hendler, J. A. and Teall, J. L. (2016), 'Investor attention on the social web', *Journal of Behavioral Finance* **17**(1), 45–59.

Lux, T. (1995), 'Herd behaviour, bubbles and crashes', *Economic Journal* **105**, 881–896.

Lux, T. and Marchesi, M. (1999), 'Scaling and criticality in a stochastic multi-agent model of a financial markets', *Nature* **397, Feb.**(11), 498–500.

Mandelbrot, B. (1963), 'The variation of certain speculative prices', *Journal of Business* **36**, 394–419.

Marquering, W. and Verbeek, M. (2004), 'The economic value of predicting stock index returns and volatility', *Journal of Financial and Quantitative Analysis* **39**, 407–429.

Moskowitz, T., Ooi, Y. H. and Pedersen, L. H. (2012), 'Time series momentum', *Journal of Financial Economics* **104**, 228–250.

Muller, U., Dacorogna, M., Dave, R., Olsen, R., Pictet, O. and von Weizsacker, J. (1997), 'Volatilities of different time resolutions – Analyzing the dynamics of market components', *Journal of Empirical Finance* **4**, 213–239.

Newey, W. K. and West, K. D. (1987), 'A simple, positive semi-definite, heteroskedasticity and autocorrelationconsistent covariance matrix', *Econometrica* **55**, 703–708.

Oliveira, N., Cortez, P. and Areal, N. (2013), On the predictability of stock market behavior using stocktwits sentiment and posting volume, *in* 'Portuguese Conference on Artificial Intelligence', Springer, pp. 355–365.

Poterba, J. and Summers, L. (1988), 'Mean reversion in stock prices: Evidence and implications', *Journal of Financial Economics* **22**, 27–59.

Scharfstein, D. and Stein, J. (1990), 'Herd behavior and investment', *American Economic Review* **80**, 465–479.

Shiller, R. (1995), 'Conversation, information, and herd behavior', *American Economic Review* **85**, 181–185.

Shive, S. (2010), 'An epidemic model of investor behavior', *Journal of Financial and Quantitative Analysis* **45**, 169–198.

Sprenger, T. O., Tumasjan, A., Sandner, P. G. and Welpe, I. M. (2014), 'Tweets and trades: The information content of stock microblogs', *European Financial Management* **20**(5), 926–957.

Welch, I. (2000), 'Herding among security analysts', *Journal of Financial Economics* **58**, 369–396.

Zhou, G. and Zhu, Y. (2014), An equilibrium model of moving-average predictability and time-series momentum, working paper, Washington University in St. Louis.

Appendix A. Proofs

A.1. **Proof of Corollary 3.1.** It is easy to verify that system (32) has a unique steady state $m_0^* = 0$ when $\beta J < 1$ and has three steady states $m_+^* > 0$, $m_0^* = 0$ and $m_-^* < 0$ when $\beta J > 1$.

When $\beta J < 1$, we rewrite (32) as

$$\frac{dm_t}{dt} = \beta J m_t \frac{\tanh(\beta J m_t)}{\beta J m_t} - m_t. \tag{A.1}$$

Applying variation of constants to (A.1), we have

$$m_t = m_0 e^{\left[\int_0^t \beta J \frac{\tanh(\beta J m_s)}{\beta J m_s} - 1\right] ds}. \tag{A.2}$$

As $t \to \infty$,

$$|m_t| = |m_0| e^{\int_0^t \left[\beta J \frac{\tanh(\beta J m_s)}{\beta J m_s} - 1\right] ds} \leq |m_0| e^{\int_0^t (\beta J - 1) ds} = |m_0| e^{(\beta J - 1)t} \to 0. \tag{A.3}$$

Therefore, $m_0^* = 0$ is globally stable.

When $\beta J > 1$, the characteristic equation of system (32) at m^* is given by

$$x - \{[1 - \tanh^2(\beta J m^*)]\beta J - 1\} = 0. \tag{A.4}$$

It is easy to verify that the eigenvalue x is positive when $m^* = m_0^*$ and negative when $m^* = m_+^*$ and $m^* = m_-^*$. This completes the proof. $\square$

A.2. **Proofs of Propositions 5.1 and 5.2.** Proposition 5.1 is a special case of Proposition 5.2. Note that

$$\langle P_t - P_{t-\tau}, P_{t+\tau} - P_t \rangle = \langle P_t, P_{t+\tau} \rangle - \langle P_t, P_t \rangle - \langle P_{t-\tau}, P_{t+\tau} \rangle + \langle P_{t-\tau}, P_t \rangle. \tag{A.5}$$

It suffices to calculate the autocovariance of $\langle P_t, P_{t+\tau} \rangle$ for all $\tau \geq 0$. It follows from (12) and (13) that

$$\begin{aligned} \langle P_t, P_{t+\tau} \rangle = & \frac{\langle D_t, D_{t+\tau} \rangle}{r^2} + \frac{1}{r\lambda}\Big(\frac{1}{r} - \frac{1}{r+\lambda}\Big)[\langle D_t, \phi_{t+\tau} \hat{f}^A_{t+\tau} + (1-\phi_{t+\tau})\hat{f}^B_{t+\tau} \rangle + \\ & \langle \phi_t \hat{f}^A_t + (1-\phi_t)\hat{f}^B_t, D_{t+\tau} \rangle] \\ & + \frac{1}{\lambda^2}\Big(\frac{1}{r} - \frac{1}{r+\lambda}\Big)^2 \langle \phi_t \hat{f}^A_t + (1-\phi_t)\hat{f}^B_t, \phi_{t+\tau}\hat{f}^A_{t+\tau} + (1-\phi_{t+\tau})\hat{f}^B_{t+\tau} \rangle \end{aligned} \tag{A.6}$$

where

$$
\begin{aligned}
&\langle D_t, D_{t+\tau}\rangle = \sigma_D^2 t,\\
&\langle D_t, \phi_{t+\tau}\hat{f}^A_{t+\tau} + (1-\phi_{t+\tau})\hat{f}^B_{t+\tau}\rangle = [\phi_{t+\tau}\gamma_A + (1-\phi_{t+\tau})\gamma_B]\frac{e^{-\lambda\tau}}{\lambda}(1-e^{-\lambda t}),\\
&\langle \phi_t\hat{f}^A_t + (1-\phi_t)\hat{f}^B_t, D_{t+\tau}\rangle = [\phi_t\gamma_A + (1-\phi_t)\gamma_B]\frac{1}{\lambda}(1-e^{-\lambda t}),\\
&\langle \phi_t\hat{f}^A_t + (1-\phi_t)\hat{f}^B_t, \phi_{t+\tau}\hat{f}^A_{t+\tau} + (1-\phi_{t+\tau})\hat{f}^B_{t+\tau}\rangle\\
&= \frac{e^{-\lambda\tau}}{2\lambda}(1-e^{-2\lambda t})\Big[\frac{1}{\sigma_D^2}(\phi_t\gamma_A + (1-\phi_t)\gamma_B)(\phi_{t+\tau}\gamma_A + (1-\phi_{t+\tau})\gamma_B)\\
&+ \sigma_f^2(\phi_t\rho_A + (1-\phi_t)\rho_B)(\phi_{t+\tau}\rho_A + (1-\phi_{t+\tau})\rho_B)\Big].
\end{aligned}
\tag{A.7}
$$

Therefore, the autocovariance $\langle P_t, P_{t+\tau}\rangle$ is given by (41), where

$$
\begin{aligned}
\Phi &= (1-e^{-\lambda\tau})\{[\phi_{t+\tau}\gamma_A + (1-\phi_{t+\tau})\gamma_B]e^{-\lambda\tau} - [\phi_t\gamma_A + (1-\phi_t)\gamma_B]\},\\
\Psi_1 &= [\phi_{t+\tau}\gamma_A + (1-\phi_{t+\tau})\gamma_B]e^{-\lambda\tau} - [\phi_t\gamma_A + (1-\phi_t)\gamma_B],\\
\Psi_2 &= (1-e^{-2\lambda t})[\phi_t\gamma_A + (1-\phi_t)\gamma_B] - (e^{-\lambda\tau} - e^{-2\lambda t+\lambda\tau})[\phi_{t-\tau}\gamma_A + (1-\phi_{t-\tau})\gamma_B],\\
\Psi_3 &= \rho[1+\epsilon(2\phi_{t+\tau}-1)]e^{-\lambda\tau} - \rho[1+\epsilon(2\phi_t-1)],\\
\Psi_4 &= (1-e^{-2\lambda t})\rho[1+\epsilon(2\phi_t-1)] - (e^{-\lambda\tau} - e^{-2\lambda t+\lambda\tau})\rho[1+\epsilon(2\phi_{t-\tau}-1)].
\end{aligned}
$$

□

As an implication, when τ is small, $e^{-\lambda\tau} \to 1$. We have the following results for (A.6):

$$
\begin{aligned}
&\Phi \to 0,\\
&\Psi_1 > 0 \Leftrightarrow \phi_{t+\tau} < \phi_t,\\
&\Psi_2 > 0 \Leftrightarrow \phi_t < \phi_{t-\tau},\\
&\Psi_3 > 0 \Leftrightarrow \phi_{t+\tau} > \phi_t,\\
&\Psi_4 > 0 \Leftrightarrow \phi_t > \phi_{t-\tau},
\end{aligned}
\tag{A.8}
$$

and hence

$$
\begin{aligned}
&\Psi_1\Psi_2 > 0 \Leftrightarrow (\phi_{t+\tau} - \phi_t)(\phi_t - \phi_{t-\tau}) > 0,\\
&\Psi_3\Psi_4 > 0 \Leftrightarrow (\phi_{t+\tau} - \phi_t)(\phi_t - \phi_{t-\tau}) > 0.
\end{aligned}
\tag{A.9}
$$

Therefore, the autocovariance is positive for small horizons if there is strong social interaction. In this case, ϕ_t keeps the same trend in a period of 2τ: $(\phi_{t+\tau} - \phi_t)(\phi_t - \phi_{t-\tau}) > 0$.

If τ is sufficiently large, then $e^{-\lambda\tau} \to 0$ and hence

$$
\Phi < 0, \qquad \Psi_1 < 0, \qquad \Psi_2 > 0, \qquad \Psi_3 > 0, \qquad \Psi_4 < 0. \tag{A.10}
$$

The autocovariance in this case becomes negative.

Appendix B. Conditional Volatility

We write the difference $\sigma_t^2 - (\sigma^*)^2$ as a function of the population fraction ϕ_t as follows:

$$f(\phi_t) := (\sigma_t)^2 - (\sigma^*)^2 = \hat{a}\phi_t^2 + \hat{b}\phi_t + \hat{c}, \tag{B.1}$$

where

$$\begin{aligned}
\hat{a} &= \frac{(\gamma_A - \gamma_B)^2 + \sigma_f^2\sigma_D^2(\rho - \rho_B)^2}{r^2(r+\lambda)^2\sigma_D^2}, \\
\hat{b} &= \frac{2\gamma_B(\gamma_A - \gamma_B) + 2(\gamma_A - \gamma_B)(r+\lambda)\sigma_D^2 + 2\sigma_f^2\sigma_D^2\rho_B(\rho_A - \rho_B)}{r^2(r+\lambda)^2\sigma_D^2}, \\
\hat{c} &= \frac{(\gamma_B - \gamma)^2 + 2(\gamma_B - \gamma)(r+\lambda)\sigma_D^2 + \sigma_f^2\sigma_D^2(\rho_B^2 - \rho^2)}{r^2(r+\lambda)^2\sigma_D^2}.
\end{aligned} \tag{B.2}$$

The axis of symmetry of the parabola in (B.1) is $-b/2a > 0$ and

$$\begin{aligned}
f(0) &= 2\sigma_D^4 r\Big[\sqrt{\lambda^2 + (1-\rho_B^2)\sigma_f^2/\sigma_D^2} - \sqrt{\lambda^2 + (1-\rho^2)\sigma_f^2/\sigma_D^2}\Big], \\
f(1) &= 2\sigma_D^4 r\Big[\sqrt{\lambda^2 + (1-\rho_A^2)\sigma_f^2/\sigma_D^2} - \sqrt{\lambda^2 + (1-\rho^2)\sigma_f^2/\sigma_D^2}\Big].
\end{aligned} \tag{B.3}$$

Thus, $f(0)$ ($f(1)$) is positive when $\rho_B < \rho$ ($\rho_A < \rho$). According to the properties of the parabola, we have the following observations:

(i) if $\rho_B < \rho < \rho_A$, then $\sigma_t^2 - (\sigma^*)^2$ is positive for a small ϕ_t closer to 0 and becomes negative for a large ϕ_t closer to 1;

(ii) if $\rho \le \rho_B < \rho_A$, then $\sigma_t^2 - (\sigma^*)^2$ is always negative for all $\phi_t \in [0,1]$;

(iii) if $\rho_B < \rho_A \le \rho$, then $\sigma_t^2 - (\sigma^*)^2$ is positive for either a small ϕ_t closer to 0 or a large ϕ_t closer to 1. When $\rho - \rho_A$ is sufficiently large, $\sigma_t^2 - (\sigma^*)^2$ becomes positive for all $\phi_t \in [0,1]$.

Fig. B.1 clearly illustrates $\sigma_t^2 - (\sigma^*)^2$ for the above three cases. Consistent with observation (iii), only when $\rho - \rho_A$ is sufficiently large do we obtain $\sigma_t^2 > (\sigma^*)^2$ for all $\phi_t \in [0,1]$. In summary, asset returns are more likely to exhibit excess volatility when investors on average underreact to the signal process. In fact, investors underreact to the signal when they are doubtful about its information value, which leads them to overreact to innovations in the dividend process due to overstating the posterior variance γ_i ($i = A, B$). As a result, asset returns become more volatile.

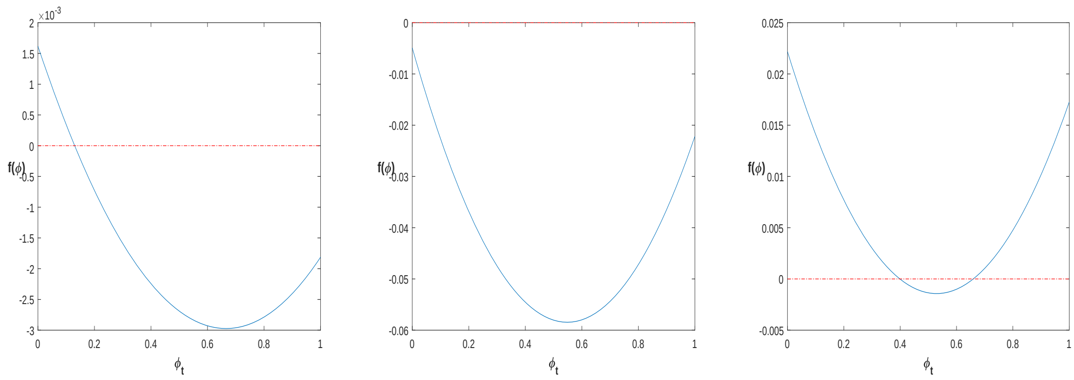

(a) $\rho_B < \rho < \rho_A$ (b) $\rho \leq \rho_B < \rho_A$ (c) $\rho_B < \rho_A \leq \rho$

FIGURE B.1. Parabola (B.1). Here $r = 0.05$, $\lambda = 0.01$, $\sigma_D = 0.05$, $\sigma_f = 0.05$ and (a) $(\rho_A, \rho_B, \rho) = (0.55, 0.45, 0.5)$, (b) $(\rho_A, \rho_B, \rho) = (0.8, 0.4, 0.1)$, and (c) $(\rho_A, \rho_B, \rho) = (0.4, 0.1, 0.8)$.

We now focus on cases $\rho_A = \rho(1+\epsilon)$ and $\rho_B = \rho(1-\epsilon)$ and numerically show that strong social interaction can lead to *excess volatility*. Fig. B.2 plots the price volatility across 100 simulations as a function of the level of social interaction J, belief disparity ϵ and sensitivity of private utility to belief accuracy b.

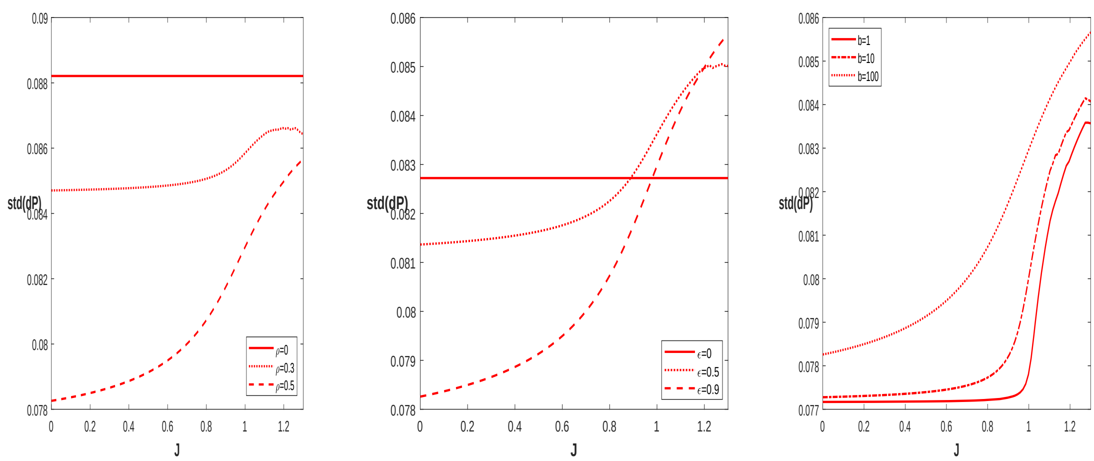

FIGURE B.2. Standard deviation of dP as functions of J for different values of (a) ρ, (b) ϵ and (c) b based on 100 simulations. The parameters are given by Table 1.

There are several observations from Fig. B.2. First, a common feature across all three panels is that the standard deviation increases more significantly in parameter J when it exceeds the threshold of 1. Intuitively, price volatility is affected by fluctuations in $\hat{f}_t^i$ and hence the mean choice. When $\beta J > 1$, due to the persistence of multiple steady states, the market sentiment and hence ϕ_t can experience large swings over time between the two regimes; thus, price volatility increases.

Second, the left panel shows that price volatility decreases in the true informativeness ρ. Note that when $\rho = 0$, all investors believe that the public signal is pure noise; thus, price volatility is given by (37). As ρ increases, the public signal becomes more informative about the fundamental, which resolves uncertainty and thus reduces price volatility.

Third, the middle panel shows a very interesting phenomenon. When social interaction is weak ($\beta J \leq 1$), a larger dispersion in interpretations about informativeness offsets the effects of these beliefs and reduces price volatility. However, the opposite is true when social interaction is strong ($\beta J > 1$): a larger dispersion between ρ_A and ρ_B makes prices more volatile. Finally, the right panel of Fig. B.2 shows that an increase in the sensitivity (b) to private utility also increases excess volatility, particularly with strong social interaction (as indicated in Fig. 1).